

# Dynamics Characteristics of the electrojet during intense magnetic disturbances

Liudmila I. Gromova<sup>1</sup>, Matthias Förster<sup>2,3</sup>, Iakov I. Feldstein<sup>1</sup>, and Patricia Ritter<sup>2</sup>

<sup>1</sup>Institute of Terrestrial Magnetism, Ionosphere, and Radiowave Propagation of the Russian Academy of Sciences (IZMIRAN), 142090 Troitsk, Moscow region, Russia

<sup>2</sup>Helmholtz-Centre Potsdam, GFZ German Research Centre for Geosciences, 14473 Potsdam, Germany

<sup>3</sup>Max-Planck-Institut für Sonnensystemforschung, 37077 Göttingen, Germany

Correspondence to: M. Förster  
mfo@gfz-potsdam.de

**Abstract.** Hall current variations in different time sectors during six magnetic storms of the summer seasons in 2003 and 2005 are examined ~~in detail~~: three storms in the day-night meridional sector and three storms in the dawn-dusk sector. ~~We investigate~~ The sequence of the phenomena, their structure, positions and the ~~density strength~~ of the polar (PE) and the auroral (AE) Hall electrojets ~~were investigated~~ using scalar magnetic field measurements obtained from the CHAMP satellite in accordance with the study of Ritter et al. (2004a). ~~Particular attention is devoted to the spatial-temporal behaviour of the PE at ionospheric altitudes during daytime hours both under geomagnetically quiet and under magnetic storm conditions.~~ We analyzed the correlations of the PE and AE ~~with various activity indices like SYM/H SymH and ASYM/H AsyH, that stand for large-scale current systems in the magnetosphere, AL for ionospheric currents, and the IndN coupling function for the state of the solar wind.~~ as well as the ~~We obtained~~ regression relations of the magnetic latitude MLat and the electrojet current ~~density intensity~~  $I$  with ~~those indices and with the interplanetary By and Bz magnetic field components.~~ auroral and ring current activity, the interplanetary magnetic field, and the Newell et al. (2007) coupling function for the state of the solar wind. ~~For the geomagnetic storms during summer seasons investigated here, we obtain~~ The following typical characteristics ~~for~~ of the electrojets ~~dynamics~~ were revealed:

1. The PE appears at magnetic latitudes (MLat) and local times (MLT) of the cusp position.
2. This occurs in the daytime sector at MLat  $\sim 73^\circ$ – $80^\circ$  with a westward or an eastward direction, depending on the orientation of the IMF By component. Changes of current flow direction in the PE can occur repeatedly during the storm, but only due to changes of the IMF By orientation.
3. The current density in the PE increases with the intensity of the IMF By component from  $I \sim 0.4$  A/m for  $B_y \sim 0$  nT up to  $I \sim 1.0$  A/m for  $B_y \sim 23$  nT.

. 4. The MLat position of the PE does not depend on the orientation and the strength of the IMF By component. It depends, however, on the strength of the IMF Bz component.

25 . 5. The PE is situated at MLat $\sim 73^\circ$  on the dayside during geomagnetically quiet periods and the recovery phase of a magnetic storm, and it shifts equatorward during intense substorms and the main phase of a storm.

. 6. There is no connection between MLat and the current density  $I$  in the PE with the magnetospheric ring current DR (index SYM/H SymH).

30 . 7. There is a correlation between the current density  $I$  in the PE and the partial ring current in the magnetosphere (PRC, index ASYM/H AsyH), but practically no correlation of this index with MLat of the PE.

. 8. Substorms that occur before and during the beginning of a storm main phase are accompanied in the daytime by the appearance of an eastward electrojet (EE) at MLat $\sim 64^\circ$ , and then also by a westward electrojet (WE). In the nighttime sector the WE appears at MLat $\sim 64^\circ$ .

35 . 9. During the development of the main storm phase, the daytime EE and the nighttime WE shift toward subauroral latitudes of MLat $\sim 56^\circ$  and intensify up to  $I \sim 1.5$  A/m. Both electrojets persist during the main phase of the storm. The WE is then located about  $6^\circ$  closer to the pole than the EE during evening hours and about  $2^\circ$ – $3^\circ$  during daytime hours.

The PE appears in the daytime sector at MLat $\sim 80^\circ$ – $73^\circ$  with a westward or an eastward direction depending on the IMF By component ( $B_y < 0$  nT or  $B_y > 0$  nT). Changes of the current flow direction  
40 in the PE can occur repeatedly during the storm, but only due to changes of the IMF By orientation. The PE increases with the intensity of the IMF By component from  $I \sim 0.4$  A/m for  $B_y \sim 0$  nT up to  $I \sim 1.0$  A/m for  $B_y \sim 23$  nT. The MLat position of the PE does not depend on the direction and intensity of the By component.

There is no connection between MLat and  $I$  in the PE with the symmetric part of the magne-  
45 tospheric ring current (index SYM/H SymH). There is a correlation between  $I$  in the PE and the ASYM/H AsyH index, but only a very weak interconnection of this index with the MLat of the PE.

Substorms occurring during daytime before the storm main phase are accompanied by the appearance of an eastward electrojet (EE) at MLat $\sim 64^\circ$  and then also of a westward electrojet (WE). In the nighttime sector, a WE appears at MLat $\sim 64^\circ$ . During the main phase both electrojets persist.  
50 The daytime EE and the nighttime WE shift toward subauroral latitudes of MLat $\sim 56^\circ$  and grow in intensity up to  $I \sim 1.5$  A/m. The WE is then located about  $6^\circ$  closer to the pole than the EE during evening hours and about  $2^\circ$ – $3^\circ$  during daytime hours.

**Keywords.** high-latitude magnetic variations, magnetic storm phases, interplanetary magnetic field, Hall current modelling, equivalent ionospheric currents, current systems in the magnetosphere, polar  
55 electrojet, eastward and westward auroral electrojets, SYM/H SymH, ASYM/H AsyH, AL, IndN

## 1 Introduction

The pioneering work of Dungey (1961) about the open nature of the magnetosphere and the role of magnetic reconnection processes between the interplanetary magnetic field (IMF) and the geomagnetic main field paved the way for the understanding of the large-scale structure and dynamics of the Earth's space environment. It provided the theoretical framework for subsequent successful investigations to understand the solar wind–magnetosphere–ionosphere–thermosphere coupling processes over several decades (Cowley, 2015).

The reconnection processes on the dayside give rise to open magnetic flux areas, the polar caps, and together with the nightside reconnections they are driving a large-scale internal magnetospheric plasma convection and current systems that connect magnetospheric and ionospheric domains. Due to the large variability of the solar wind and IMF conditions, the whole system is very dynamic and the amount of open flux in the polar cap changes continuously. The theoretical understanding of the polar cap formation and its time evolution was advanced to the fully time-dependent “expanding/contracting polar cap” (ECPC) paradigm by the work of Cowley and Lockwood (1992). A comprehensive review of all the aspects of the magnetosphere-ionosphere-thermosphere interaction processes under the solar wind driver was provided recently by Milan (2015).

The principal pattern of the large-scale field-aligned current (FAC) system, also known as Birkeland currents, which form circumpolar belts of Region-1 (on the poleward side) and Region-2 FACs (on the equatorward side) was disclosed by the work of Iijima and Potemra (1976a). On the dayside adjacent to the cusp region, so-called Region-0 FACs are observed (Iijima and Potemra, 1976b). Using MAGSAT satellite data, Iijima et al. (1984) showed in the dayside sector of the polar cap the existence of a particular FAC system, the so-called NBZ Birkeland currents for intervals of positive IMF  $B_z$ .

From ground-based magnetometer observations, the high-latitude electrojets have been studied already prior to the space era (cf., e.g., Chapman and Bartels, 1940). The particularities of high-latitude ionospheric current systems during magnetic disturbances were known empirically (Chapman, 1935). Levitin et al. (1982) revealed high-latitude current systems for summer conditions, which are controlled by the IMF components and solar wind parameters. Based on such equivalent current systems and considering informations about the anisotropic ionospheric conductivity, Friis-Christensen et al. (1985) showed the possibility to determine a full current system, including FACs and horizontal currents in the ionosphere. Such a full current system can be estimated as a combination of the equivalent currents obtained both from ground-based and satellite observations of the magnetic variations (Green et al., 2007).

An intense study of the polar electrojet (PE) at the high-latitude daytime ionosphere was initiated by the works of Svalgaard (1968) and Mansurov (1969). They had demonstrated that its characteristic magnetic field variation depends on the sector structure of the ~~interplanetary magnetic field (IMF)~~ that is much alike the average magnetic field of the solar photosphere. ~~The IMF lines up in a spiral structure near the ecliptic plane with IMF  $B_x > 0$  and  $B_y < 0$  (toward the sun) or  $B_x < 0$  and~~

~~By > 0 (away from the sun), where one prevalent direction is kept usually for several days. During summer the sector structure is accompanied by intense variations of the geomagnetic Z component within the polar cap at  $\Phi \sim 86^\circ$  and of the H component at  $\Phi \sim 78^\circ$ . An increase or decrease of the magnetic field components with respect to the quiet time is determined by the activity level and the IMF sector structure.  $\Delta Z < 0$  and  $\Delta H > 0$  is found for the away sector, and the opposite variations for the toward sector.~~ The IMF sector structure does not always correspond to the expected magnetic

field variations in the near-polar region. Friis-Christensen et al. (1972) showed that during periods of discrepancy between the expected magnetic variations and the sector structure from satellite observations, there existed always an essential deviation of the IMF from the usual spiral structure. During these cases, the azimuthal IMF By component was oppositely directed to the expected direction of the spiral. This implies, that the magnetic variation on ground is not primarily controlled by the sector structure (toward or away the sun), but by the azimuthal component of the IMF (eastward or westward).

Various methods have been developed for the extraction of the PE magnetic field variations from groundbased observations in the near-polar region (Feldstein, 1976). The most effective approach appeared to be the correlation method (Jørgensen et al., 1972; Friis-Christensen and Wilhjelm, 1975; Feldstein et al., 1975b). It is based on the fact, that both the direction of the PE and its intensity depend on the IMF By component. The method allows to separate the magnetic variations of the PE from variations of other sources and to show the spatial-temporal variation of the PE vector variations very clearly. Feldstein et al. (1975b) described the findings of a geomagnetically quiet interval in summer 1965 and the characteristics of the equivalent current system, controlled by the IMF By component. In a first step, time intervals with correlations of the magnetic X(H), Y, and Z components with IMF By were identified for observatories with  $\Phi > 65^\circ$ . In case of existing correlations, they appeared to be practically always close to a linear dependence with a correlation coefficient  $r$ . Correlation was assumed to exist for values of  $r > 0.4$ ; otherwise (for  $r \leq 0.4$ ) it was assumed as non existing. Such a boundary for significant  $r$  values is justified by the correlation correction  $S_r = (1 - r^2) / \sqrt{n - 1}$ . For values of  $|r/S_r| \geq 3$ , the relation between the X(H), Y, and Z components with the IMF By cannot be regarded as accidental. With  $n \sim 50$  the correlation is not randomly distributed for  $r > 0.4$ .

Regression lines, which relate the ground magnetic variations with the IMF By component, were estimated for all MLT, based on the observed intervals with  $r > 0.4$ . They were used to describe the spatial-temporal distribution of the **surface** magnetic variations in the horizontal and vertical plane, and finally for the estimation of the equivalent current system for IMF By = 6 nT. Its integral intensity amounts to 180 kA with a maximum current density of the electrojet in the dayside sector of  $\sim 0.5 A/m$  at  $80^\circ < \Phi < 81^\circ$ . An analogous estimation for July-August 1966 resulted in a value of  $\sim 0.35 A/m$  at the same latitudes (Sumaruk and Feldstein, 1973).

The PE in the dayside sector does not disappear during magnetic disturbances (Feldstein et al.,

2006). The PE shifts equatorward to  $72^\circ < \Phi < 74^\circ$  in the longitudinal range of  $08 < \text{MLT} < 17$  during intense substorms (with  $\text{AL} \sim -800$  nT), and during periods of geomagnetic storms with  $\text{AL} \sim -1200$  nT and  $\text{Dst} \sim -150$  nT it is situated at  $66^\circ < \Phi < 68^\circ$  between  $09 < \text{MLT} < 15$ . The current intensities of the PE increases only slightly to about  $\sim 0.5$  A/m.

135 The variations of the magnetic field at the Earth's surface at high latitudes, which were derived with the method of regression analysis, allowed to determine the IMF By control of the spatial-temporal distributions of the electric field potential at ionospheric altitudes as well as the ionospheric and field-aligned currents (FACs) (Friis-Christensen et al., 1985; Feldstein and Levitin, 1986). The electric field potential for an inhomogeneous ionospheric conductivity is obtained by solving a  
140 second-order partial differential equation. Friis-Christensen et al. (1985) used magnetic observations of the summer seasons in 1972 and 1973, while Feldstein and Levitin (1986) obtained it for summer 1968. The potential differences at cusp latitudes in the daytime sector are  $\sim 20$  kV for IMF By  $\sim \pm 6$  nT.

~~Leontyev and Lyatsky (1974) postulated a penetration of the solar wind electric field into the magnetosphere at daytime cusp latitudes. This electric field is generated by the potential difference between the northern and southern boundaries of the magnetotail. Under the assumption of high conductivities along the magnetic field lines, the electric field exists only at open field lines, which have their footprints in the polar caps, and will be short-circuited along closed field lines. The model allowed to estimate the effectivity of the solar wind electric field penetration into the magnetosphere to  $\sim 10\%$ .~~

150 Olsen (1996) used MAGSAT magnetic field data in a height range of  $350 < h < 550$  km to determine the strength and location of the auroral electrojets at 115 km altitude. He showed for the first time the possibility to estimate the horizontal ionospheric currents from scalar magnetic measurements only. The ionospheric currents were modelled by hundreds of infinite linear currents perpendicular to the orbital plane of the spacecraft with discretisation intervals of 111 km. The problem of  
155 ionospheric current estimation is underdetermined and its solution is not unique. In order to constrain the solution, a regularization method is used. The ~~compilation~~ comparison of modelled and measured variations of the magnetic field along the satellite orbit on December 04, 1979, 17:00 UT, demonstrateds the good agreement for the field-aligned component, but a significant discrepancy for  
160 the field-perpendicular one. The discrepancy is mainly caused by magnetic fields of the FACs. The integral amplitude of the ionospheric currents during the interval November 28 till December 10, 1979, yielded a correlation of  $r = 0.88$  with the AE-index.

The IMF By orientation influences not only the PE, but also the movements of the auroral forms at cusp latitudes (Sandholt et al., 2002). Simultaneously with permanently poleward moving discrete auroral forms at the equatorward boundary of the cusp, which are controlled by the IMF Bz component, there exist east-west moving auroral forms. This azimuthal movement is controlled  
165 by IMF By, such that for  $\text{By} > 0$  the discrete forms move westward and for  $\text{By} < 0$  eastward. The

movement of the auroral forms is in opposite direction to the PE current flow direction. This can be expected, because the discrete auroral forms and the channels of enhanced ionospheric conductivity are both due to precipitating electrons into the upper atmosphere. A detailed consideration of the interrelation between auroral luminosity, auroral particle precipitation, and the PE during magnetic disturbances was given by Sandholt et al. (2004). As shown there, the strong convection channel is located on the dawn side of the polar cap for IMF  $B_y > 0$ , and on the dusk side for  $B_y < 0$  conditions. The electron precipitation in the regime of the convection channel in the morning sector consists of a band ( $\sim 500$  km) of structured precipitation. The PE is located on the high-latitude boundary of the structured luminosity region in the vicinity of the strong flow channel of magnetospheric convection close to the bright auroral arc. For  $B_y > 0$ , this channel is located in the morning sector on the poleward side of the polar cap boundary with FAC out of the ionosphere, and FAC into the ionosphere equatorward of the polar cap boundary.

Ritter et al. (2004b) investigated variations in the location and density strength of the auroral electrojets, which were independently determined both from ground-based (IMAGE magnetometer network) and satellite (CHAMP) measurements. ~~For the estimation of the Hall current from CHAMP data, a current model consisting of a series of 160 current lines were placed at an altitude of 110 km and separated by  $1^\circ$  in latitude. The magnetic field of the line currents were related to the current strength  $I$  according to the Biot-Savart law. The density strength of each of the 160 line currents were derived from an inversion of the observed field residuals using a least-square fitting approach. They determined the geomagnetic latitude and current densities of the eastward (EE) and westward electrojets (WE) in the evening, nighttime, and morning sectors. Two or one-dimensional ionospheric Hall current systems were independently determined from variations of the horizontal magnetic field, measured by the IMAGE ground-based magnetometer network. Comparisons of satellite with ground-based measurements of ionospheric currents at auroral latitudes have been done for satellite passages during magnetic storms as, e.g., that of 5–6 November 2001, during substorms, and according to statistical data. The ratio of the current densities from IMAGE and CHAMP was provided for a latitudinal range of  $60^\circ$ – $77^\circ$  as well as mean values of the current densities, variations of the correlation coefficients, and coefficients of the regression equations. The ratio of the current densities and of the correlation coefficient as determined from currents above and below the ionosphere, is close to unity. Such a correspondence between the results of two different model approaches constitute the base for the following statements: a) the estimation of the position and density strength of the auroral electrojets can be carried out with observations above the ionospheric current layer by means of low-Earth orbiting (LEO) satellites; b) the currents can be estimated from scalar magnetic field measurements; c) the result of the calculations are the parameters of the Hall current at an altitude of  $\sim 110$  km (where the maximum value of the ionospheric Hall conductivity occurs). This method of Hall current estimation from satellites was proposed for the first time by Olsen (1996). Its detailed justification has been validated quantitatively by ground-based~~

205 observations by Ritter et al., 2004b.

~~Based on magnetometer data of the IMAGE and EISCAT networks, Feldstein et al. (1997) showed that the electrojets shift equatorward during the main phase of strong magnetic storms. For  $DST \sim -300$  nT, the EE in the evening and the WE in the nighttime and early morning hours shifts to  $\sim 54^\circ \sim 55^\circ$ . Feldstein and Galperin (1999) studied the correlation between EE and WE with the structure of plasma precipitations of 30 eV–30 keV according to DMSP F08, F10, and F11 satellite observations during the magnetic storms of 10–11 May 1992, 05–07 February 1994, and 21–22 February 1994. The EE displaces in the region of diffuse aurora, equatorward of the discrete auroral forms, and projects along magnetic field lines into the inner magnetosphere between the plasmasphere and the central plasma sheet of the magnetospheric tail. The WE is located at the auroral oval and projects along magnetic field lines toward the central plasma sheet in the tail.~~

210

215

Wang et al. (2008) made use of the Hall current estimations for the intense magnetic storms of 31 March to 01 April 2001 and 17–21 April 2002 to investigate the position and current densities of auroral electrojets (WE and EE) as well as the relations of the electrojets to the Dst index and the IMF Bz component. ~~The characteristics of the PE have not been considered by these authors.~~ The currents were determined from scalar magnetic field measurements of the CHAMP satellite (orbit in the meridional plane of 15–03 MLT and 16–04 MLT) according to the method ~~that was proposed by~~ of Ritter et al. (2004b). ~~The intensity of the WE on the nightside is on average two time larger than the EE on the dayside.~~

220

In this study we investigate not only the auroral electrojet, but also the polar electrojet characteristics during six intense magnetic summer storms. ~~In this introduction section we have briefly described the historic progression of method used to determine the ionospheric currents from space observations with LEO satellites and from ground magnetic field data.~~ In section 2 we present an overview of the CHAMP data used as well as the indices, which characterize the electro-magnetic conditions in the near-Earth space during the geomagnetic storms under study. Section 3 provides a short description of the method for the determination of the Hall currents from CHAMP scalar magnetic records. In section 4 we consider the latitudinal variation of the ~~density strength~~ and position of the electrojets during different phases of the magnetic storm on 29–30 May 2003. Particular attention is drawn to the polar electrojet (PE). ~~The subsequent section 5 provides detailed correlation analyses and~~ the discussion of the control of the current direction in the electrojets, its ~~density strength and latitudinal position. by various indices, which characterize the disturbance level and the effectivity of the interaction of the interplanetary medium on the magnetospheric processes follows in the subsections 5.1 and 5.2 for the polar electrojet (PE) and the auroral electrojets (AE), respectively.~~ The Conclusion's section 6 summarizes the main results of the study with respect to the Hall current variations during the various storm phases ~~(subsection 6), the polar electrojet (6), and the auroral electrojet within four different time sectors (6).~~

225

230

235

240



**Table 1.** Overview of CHAMP satellite orbits used for this study.

Date & Time (UT, hrs)	CHAMP orbit numbers	MLT range (hrs)	
		ascending	descending
29/30 May 2003, 16–10	16229–16240	~14–16	~02–04
24 Aug 2005, 07–20	29012–29020	~11–12	~23–24
18 Jun 2003, 03–18	16532–16541	~12–16	~00–04
30 May 2005, 02–17	27658–27667	~19–21	~06–09
15 May 2005, 00–19	27423–27432	~20–22	~08–10
18 Aug 2003, 00–23	17480–17494	~07–09	~19–21

## 2 Data

The CHALLENGING Minisatellite Payload (CHAMP) spacecraft (Reigber et al., 2002) was launched on 15 July 2000 into a circular, near-polar orbit with an inclination of  $87.3^\circ$ . From its initial orbital height at  $\sim 460$  km, it has decayed to  $\sim 400$  km in 2003 and  $\sim 350$  km after 5 years. The orbital plane precesses to earlier local times at a rate of about one hour per 11 days so that the orbit covers all local times within about 131 days. The data used in this study are scalar magnetic field measurements obtained with the Overhauser Magnetometer (OVM) at the boom tip with a resolution of 0.1 nT. In order to isolate the magnetic effect of ionospheric currents in the satellite data, the contributions from all other sources have been removed from the scalar field readings as described in the study of Ritter et al. (2004a).

The CHAMP orbital intervals during various storm periods used for this study are listed in Table 1. The quantity, locations, and intensity of the peaks along the latitudinal current density intensity distribution varies over the course of the storm development. For the description of the storm development, we utilise various solar and geomagnetic indices.

First, we employ the auroral electrojet index (AE), which is derived from geomagnetic variations in the horizontal component observed at 12 selected (~~10–13~~) observatories along the auroral zone in the Northern Hemisphere (<http://wdc.kugi.kyoto-u.ac.jp/aedir/index.html>). The upper (AU) and lower envelope (AL) of the superposed plots of all the data from these stations as functions of UT is used in this study.

Further, we employ the ~~SYM/H~~ SymH and ~~ASYM/H~~ AsyH indices, which describe the geomagnetic disturbances at mid-latitudes in terms of longitudinally asymmetric (ASY) and symmetric (SYM) disturbances for the H component (<http://wdc.kugi.kyoto-u.ac.jp/aeasy/index.html> or, alternatively, [http://omniweb.gsfc.nasa.gov/ow\\_min.html](http://omniweb.gsfc.nasa.gov/ow_min.html)). ~~SYM-H~~ SymH is essentially the same as the Dst index, but with a different time resolution (1-min cadence).

Finally, Newell et al. (2007) proposed a new solar wind coupling function, representing the rate of



magnetic flux opened at the magnetopause,  $d\Phi_{MP}/dt$ , which is referred to here as Index N (IndN). It is used for the correlation analysis in the solar-terrestrial physics:

$$IndN = d\Phi_{MP}/dt = v^{4/3} B_T^{2/3} \sin^{8/3}(\theta_c/2) \quad (1)$$

Here,  $\Phi$  (or  $\Phi_{PC}$ ) is the (open) magnetic flux that constitutes the polar cap,  $v$  describes the solar wind speed or, more precisely, the transport velocity of IMF field lines that approach the magnetopause,  $B_T$  is the magnitude of the IMF,  $\sin^{8/3}(\theta_c/2)$  is the percentage of field lines, which subsequently merge, and the IMF clock angle  $\theta_c$  is defined by  $\theta_c = \arctan 2(B_y/B_z)$ . This function describes best the interaction between the solar wind and the magnetosphere over a wide variety of magnetospheric activity. IndN has a strong correlation with other indices that characterize both the plasma and the IMF in the solar wind as well as the processes in the magnetosphere. By means of a statistical study of the electrojet characteristics, the new function IndN was used together with the classical indices SYM/H SymH, ASYM/H AsyH, and AL. For the determination of all indices throughout this study we used time averages of the overflight intervals.

### 3 Method

Ionospheric currents at high latitudes, which are recorded by low-Earth orbiting (LEO) satellites as magnetic field deviations, represent the sum of FACs between the magnetosphere and ionosphere (Birkeland currents) and predominantly horizontal ionospheric currents, which flow mainly in the highly conducting ionospheric E layer below the satellite orbit.

The horizontal sheet currents are commonly decomposed in two different ways. The classical fundamental theorem of vector calculus, known as Helmholtz's theorem, states that any vector field can be decomposed into the sum of a curl-free and a divergence-free part. On the other hand, considering the relation to an electric field, the sheet current is composed of Pedersen currents, which flow in the direction transverse to the magnetic field and parallel to the electric field in the neutral wind frame of reference (e.g., Baumjohann and Treumann, 1996; Richmond, 1995), and Hall currents, which are perpendicular to both fields. The latter decomposition requires, however, the knowledge of the electric field in the neutral wind frame of reference, which is not given in our case.

Using the Helmholtz theorem, we assume the Hall currents to be divergence-free, i.e., they are supposed to close entirely within the ionosphere, while the Pedersen currents are curl-free, connecting essentially various branches of FACs. Laundal et al. (2018) showed (see their Figure 14), that during summer conditions, which is the case for the six storm intervals analysed in this study, the divergence-free and curl-free ionospheric currents are mainly represented by the Hall and Pedersen currents, respectively.

The Hall current flows at high latitudes are derived from CHAMP scalar magnetometer records along the satellite orbits according to the method that was proposed presented by Ritter et al. (2004b).

This method of Hall current estimation from scalar magnetometer records of satellites was proposed for the first time by Olsen (1996). These calculations make use of a current model consisting of a series of 160 infinite current ~~stripes~~ lines, which were placed at an altitude of 110 km and separated by  $1^\circ$  in latitude. ~~†~~ The magnetic field of ~~which corresponds to the measured values~~; the line currents were related to the current strength  $I$  according to the Biot-Savart law. The strength of each of the 160 line currents were derived from an inversion of the observed field residuals using a least-square fitting approach. The model does not take into account the contributions from field-aligned and Pedersen currents, measured at CHAMP altitudes. The comparison with ground-based geomagnetic variations of the horizontal component that considers only the contributions from the ionospheric Hall current field, because the contributions from the field-aligned and the Pedersen currents largely cancel ~~there~~ each other (Fukushima, 1976), showed the applicability with high reliability of the modelling assumptions by Ritter et al. (2004b) ~~even particularly~~ for the estimation of the Hall currents.

The ~~density level~~ of ionisation in the near noon hours at latitudes of  $75^\circ < \Phi < 80^\circ$  decreases from summer to winter season by about an order of magnitude (Feldstein et al., 1975a). The PE current ~~density strength~~ amounts during winter to  $\sim 0.1$  A/m, which makes it difficult to be measured adequately by magnetometers onboard of satellites. Because of that we investigate in this study summer storms only: three storms with CHAMP orbits in the midday-midnight plane and three in the dawn-dusk plane (listed in Table 1). ~~Here, we describe only one of these storms, namely that of May 29–30, 2003. Five of the~~ The five other storms are described in the appendix / supplementary material to this paper.

The storm phases are identified in this study according to the ~~SYM/H~~ SymH index, which describes together with the ~~ASYM/H~~ AsyH index the large-scale variations of the geomagnetic field with a 1-min cadence. In essence, ~~they~~ SymH represents ~~the~~ mean values of the magnetic field deviation from the quiet time level for a longitudinally distributed chain of ~~six~~ mid-latitude ~~observatories~~ stations. ~~The current at the magnetopause (DCF) and the currents within the magnetosphere as the ring current (DR), which is asymmetric with respect to the geomagnetic axis, and the tail current (DT), which closes via the dayside magnetopause, determine the intensity and the development of the magnetic disturbances. These currents carry the main contributions to the SYM/H values of the magnetic disturbances during magnetic storm intervals (Maltsev, 2004; Alexeev et al., 1996).~~

The ~~density intensity~~ of the ring current varies with longitude. This variability ~~is identified as the partial ring current (PRC)~~, denoted by the ~~ASYM/H~~ AsyH index, ~~and is~~ determined as the ~~difference range~~ between the maximum and minimum magnetic field values of the disturbance field minus the SymH from ~~a the~~ longitudinal chain of mid-latitude ~~observatories~~ stations. ~~The PRC current system is a 3-D one that is confined to a limited azimuthal range of the ring current in the magnetosphere, FACs between the magnetosphere and ionosphere at the border of the PRC, and an EE in the evening sector at ionospheric heights. The latitude position is controlled by MLT and toward the near noon~~

sector it shifts toward the ionospheric footpoint of the cusp region (Feldstein et al., 2006). The FAC of the PRC maps from ionospheric heights to the near-cusp magnetopause region, where the Hall currents flow, which are controlled by the IMF By component.

#### 4 The storm of 29–30 May 2003

The orbit of the CHAMP satellite in its ascending branch was on the dayside ( $\sim 14$ – $16$  MLT), while its descending branch was in the nighttime sector ( $\sim 02$ – $04$  MLT). Figure 1 shows various geomagnetic indices and the variation of the By and Bz components of the IMF during the storm progression together with the times of CHAMP satellite observations during crossings of the northern polar cap regions, indicated by dashed vertical lines. The respective CHAMP orbit numbers are given above the uppermost panel with the first three digits on the left side and the last two digits in between the two vertical dashed lines that indicate the corresponding observation intervals.

The beginning of the main magnetic storm phase was identified during orbit 16233 at 22:24 UT ( $\epsilon$  with an average SymH value of  $-61.6$  nT) for the overflight interval, while the minimum value of ~~SYM/H~~ SymH was recorded during orbit 16234 at 23:59 UT ( $-123.5$  nT) and orbit 16235 at 01:33 UT ( $-139.5$  nT). The four orbits prior to the main phase (16229–16232) at 16:18 UT–20:53 UT are characterized by ~~SYM/H~~ SymH values of  $-1.6$  nT,  $-35.6$  nT,  $-59.6$  nT, and  $-27.0$  nT as well as the occurrence of three substorms with intensities according to AL values in the range of  $\sim -1600$  nT to  $\sim -2400$  nT. ~~ASYM/H~~ AsyH increases sharply prior to the beginning of the main phase ( $208.3$  nT during orbit 16231) and during the beginning of the main phase ( $290.7$  nT during orbit 16233). In the maximum of the main phase, the values of this index decrease to  $75.5$  nT during orbit 16234 and  $145.0$  nT during orbit 16235. Following the main phase, the recovery phase develops (orbits 16236–16240) at 03:03 UT–09:21 UT, in the course of which the ~~SYM/H~~ SymH values return to the initial values at  $\sim -60$  nT and ~~ASYM/H~~ AsyH decreases to  $51$  nT during orbit 16239.

Let us now consider the structure and the latitudinal variation of the position and density strength of the electrojet during the various phases of the analysed storm. The eastward (EE) and westward electrojet (WE) can exist in the daytime sector at latitudes of the auroral zone ( $\sim 60^\circ < \text{MLat} < 70^\circ$ ), while poleward of it, at latitudes of the auroral oval ( $\sim 73^\circ < \text{MLat} < 79^\circ$ ), the currents of the polar electrojet (PE) can appear. The direction of the PE, however, can be eastward or westward. This is determined by the sign of the IMF By component: eastward current in the PE for  $B_y > 0$ , and westward for  $B_y < 0$ . In the nighttime sector, the current is westward directed (WE) in the majority of cases at auroral latitudes. Fig. 2 shows the direction, MLat, and density strength of the Hall currents along the orbit for dayside (left column) and nightside (right column) sectors as obtained from scalar measurements of the geomagnetic variations corresponding to the modelled current variations of Ritter et al. (2004b). The current direction is related to the orientation of the satellite orbit: positive currents point eastward for the descending orbital parts and westward for the ascending. The auroral

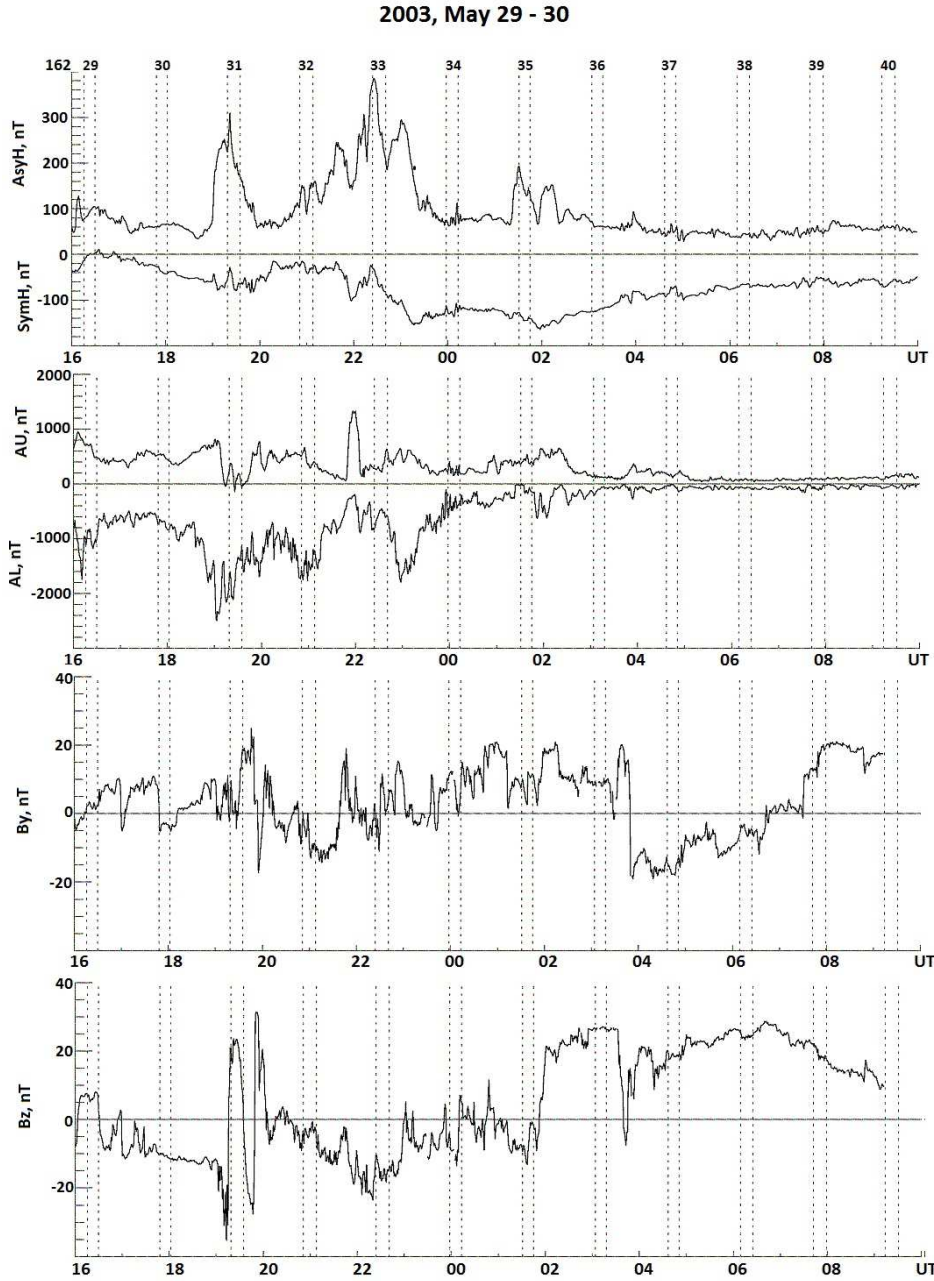


**Fig. 1.** One-minute values of the **ASYM/H** AsyH, **SYM/H** SymH, **AU**, and **AL** indices and of the  $B_y$  and  $B_z$  components of the IMF for the storm of 29–30 May 2003 (analysed interval from 16:00 UT on 29 May to 10:00 UT on 30 May 2003, orbits 16229–16240). The **paired** vertical dashed lines indicate the UT time **moments intervals** of each satellite **orbit crossing** over the northern polar cap. The orbit numbers are splitted into two parts: the two digits above the **UT-axis-of-each uppermost** frame denote the last two digits of the orbit numbers of the CHAMP passes, while the first three digits are indicated at the **lower upper** left side.

2003, May 29 - 30

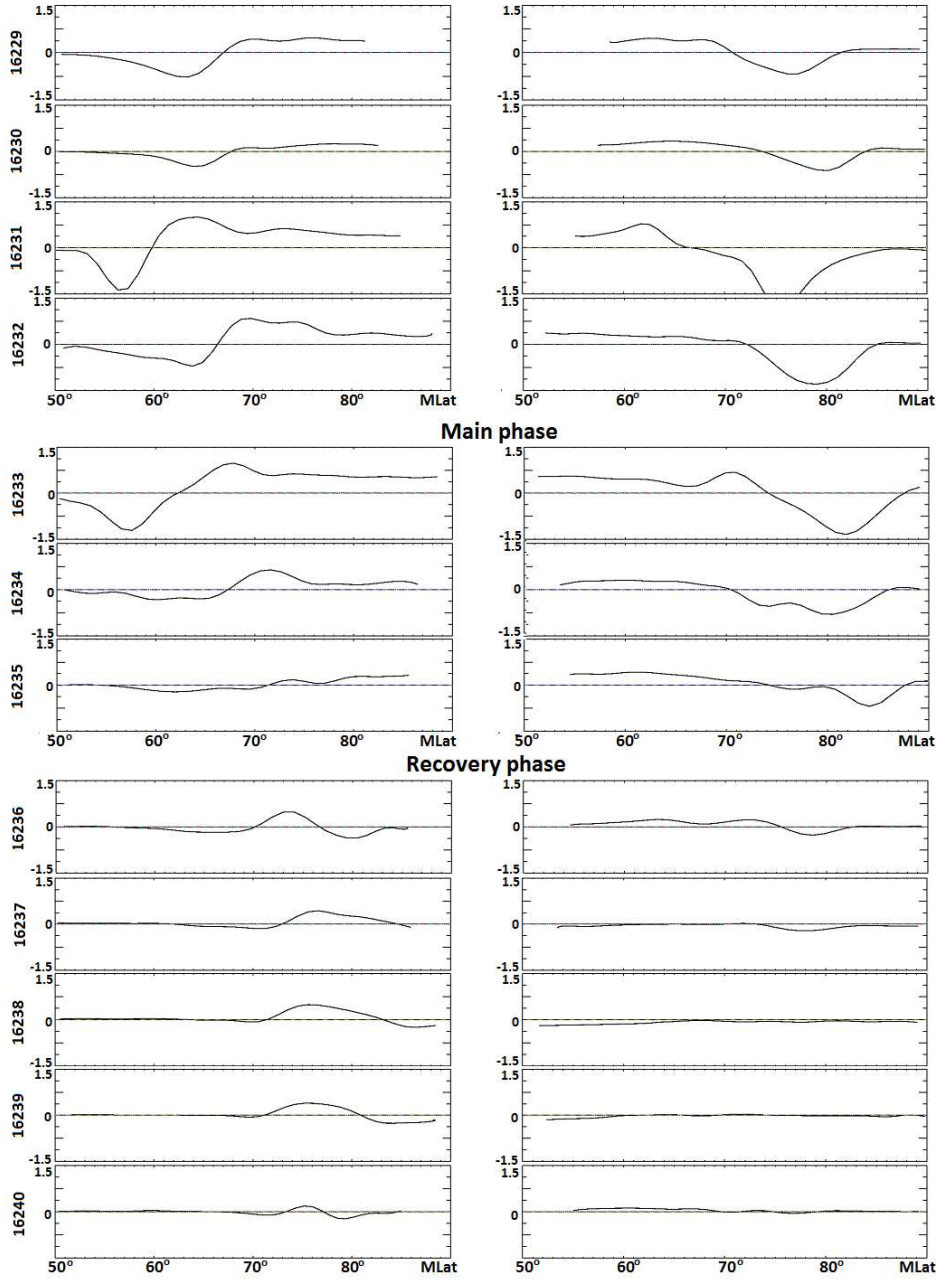


Fig. 2. Direction and **density intensity** values of the Hall current **in units of [A/m]** along the satellite orbit at the dayside (left column, 14–16 MLT, corresponding to the ascending section of the orbit) and nightside sectors (right column, 02–04 MLT, descending orbit section). Positive currents denotes eastward current for the descending orbit section, and, **accordingly**, westward current for the ascending section, **respectively**.

electrojet current flow is assumed to be in strict east-west direction due to method constraints. It is obvious that the quantity, locations, and intensity of the peaks along the latitudinal current density intensity distribution vary in the course of the storm development. A close correlation of the EE and WE can be expected for the AU and AL indices, respectively, which are regarded as a measure of the auroral electrojets from the ground. We are considering, however, magnetic records along the satellite orbit well above the ionospheric current layer.

#### 4.1 Observations related to SYM/H SymH variations

The latitudinal variation of the position and density strength of the EE is shown in Fig. 2, left panels. During the orbits 16229 and 16230, one singular peak of eastward current was observed, which occurred at MLat = 63.4° and MLat = 64.0° with intensities of 1.0 A/m and 0.6 A/m, respectively. This means that the EE peak current diminishes in density intensity with increasing disturbances according to the SYM/H SymH index and shifts to higher latitudes. During the orbits 16231–16233 (in the substorms interval and at the beginning of the main storm phase), one can clearly note two intense peaks: one of the eastward current (EE), and another of the westward current (WE - the westward electrojet). The EE peak during orbit 16231 amounts to ~1.83 A/m at MLat = 56.3°, decreasing in the course of the next orbit to 0.94 A/m at MLat = 63.9°.

With the beginning of the main phase, the current again intensifies to 1.61 A/m at MLat = 57.6°. The EE variations in density strength and latitudinal position during the orbits 16231–16233 proceed analogous to the SYM/H SymH changes: the more intense SYM/H SymH, the closer to the equator shifts the EE peak and the stronger becomes its current density intensity.

But such an accordance is broken again in the maximum of the main phase similar to orbits 1622934 and 162305: SYM/H SymH increases in intensity, while the EE in its peak diminishes to 0.44 A/m and even 0.29 A/m at MLat = 61.0°. The EE peak amounts to 0.23 A/m at MLat = 65.2° during orbit 16236 in the recovery phase and diminishes further to values <0.2 A/m during the subsequent orbits, which complicates the identification of the EE position. This way the EE follows with its varying current densities at auroral latitudes the growth (or creation) and main phases of the magnetic storm. It should be noted, that SYM/H SymH remains still significant during the recovery phase, with values of ~-60 nT. This exceeds the intensity of SYM/H SymH during the substorm interval and at the beginning of the storm main phase, while the EE during the recovery phase is much smaller than during the substorm interval.

In contrast to the EE, a westward current exists on the dayside sector during the whole interval considered, except the two first orbits, and achieves during the substorm interval values of 1.1–1.3 A/m within the peaks at 64° < MLat < 70°. It is obvious that the WE does not attain the CHAMP meridian (~14–16 MLT) during the first two orbits, while it strengthens in the nighttime sector and propagates toward the evening hours. During the orbits 16231–16233, the latitude and density strength of the WE peak changes in phase with the SYM/H SymH intensity, analogous to the current



variations in the EE peak. During the maximum of the main phase the WE peak diminishes to  
410 0.8–0.25  $A/m$  at  $71^\circ < \text{MLat} < 74^\circ$  in antiphase to **SYM/H SymH**.

The peaks of westward current remain at a level of  $\sim 0.6 A/m$  within  $73^\circ < \text{MLat} < 76^\circ$  during the recovery phase. An additional peak of eastward current with a **density strength** of  $0.49 A/m$  appears during orbit 16236 at  $\text{MLat} = 80.5^\circ$  during early afternoon hours ( $\text{MLT} \sim 14.5$  hrs). This latitude and the MLT range around midday imply that the current observed is the PE. In this case its  
415 orientation is controlled by the IMF  $B_y$  component and for an eastward PE the  $B_y$  component should be positive (Friis-Christensen et al., 1972; Sumaruk and Feldstein, 1973; Feldstein, 1976). Indeed, according to Fig. 1,  $B_y = 9 nT$  during the period of this orbit. During the two subsequent orbits, the Hall current changes its direction to westward at  $\text{MLat} \sim 80^\circ$ . If this westward current prove to be the PE, then its appearance should be connected with a change of the IMF  $B_y$  component. Indeed,  
420 the currents are accompanied with a change of sign of the IMF  $B_y$  component, corresponding to  $-17.5 nT$  ( $\text{MLat} = 80.7^\circ$ ) during orbit 16237 and  $-5.2 nT$  ( $\text{MLat} = 80.6^\circ$ ) during orbit 16238. During the orbits 16239 and 16240 the IMF  $B_y$  component turns to positive values again and weak eastward directed currents appear accordingly at  $\text{MLat} \sim 80^\circ$ .

In the majority of latitudinal profiles of the nighttime sector (Figs. 2, **right panels**), there one peak  
425 of the WE exists at latitudes of the auroral oval and some weakly spreaded eastward currents. Two orbits constitute an exception - one prior to (16231) and another during the beginning of the main storm phase (16233). These orbits pertain to the period of intense substorms. Within the polar cap up to the geomagnetic pole, there exist quite intense (up to  $0.9 A/m$ ) eastward currents.

These currents might contain irregularities, which are caused by the appearance of a peak of  
430 eastward currents in the latitudinal profile. The monotonicity of the eastward current variations within the polar cap during most orbits provides some reason to assume, that these currents result from the closure of an intense WE current, which occurs at latitudes of the auroral oval in the nighttime sector.

At the beginning of the substorm interval (orbits 16229 and 16230) with the intensification of  
435 **SYM/H SymH**, the WE peak shifts to lower latitudes and the current **density intensity** diminishes. The most intense peaks of the nighttime WE are obtained during the substorm interval prior to the main phase start with and retain values of  $2.7 A/m$  at  $\text{MLat} = 64.4^\circ$  (orbit 16231),  $1.7 A/m$  at  $\text{MLat} = 60.9^\circ$  (orbit 16232), and during the beginning of the main phase with  $1.79 A/m$  at  $\text{MLat} = 58.0^\circ$  (orbit 16233). Later in the maximum of the main storm phase, the WE peak current  
440 **density strength** diminishes to  $1.07 A/m$  at  $\text{MLat} = 59.5^\circ$  (orbit 16234) and  $0.9 A/m$  at  $\text{MLat} = 55.8^\circ$  (orbit 16235). Hence, the latitudinal peaks of the WE vary during nighttime in phase with the intensification of **SYM/H SymH** (storm development) before the main phase commences at higher latitudes, while shifting to the equator during the maximum of the main phase. The peak intensities changes both in phase and in antiphase with the **SYM/H SymH** intensity. During the recovery phase,  
445 the peak **density intensity** of the WE current is smaller than  $0.2 A/m$ , while the eastward currents



within the polar cap are too small to be recorded.

#### 4.2 Observations related to **ASYM/H AsyH** variations and to high-latitude currents

In the dayside sector during the existence of the EE (orbits 16229–16236), the peak current intensities and the peak latitude positions vary synchronous with the **ASYM/H AsyH** changes, except  
450 of one orbit (16235) during the main phase. During this orbit, the **ASYM/H AsyH** index abruptly intensifies to  $145 \text{ nT}$  with a pertaining small **density intensity** of the EE with  $\sim 0.29 \text{ A/m}$  and a shift of MLat by  $1.8^\circ$ . For the WE, the change in latitude and **density strength** of the peak currents is in phase with the **ASYM/H AsyH** variations during the storm, with the exception of orbit 16235.

In the nighttime sector, the intensity of the peaks and their latitude (except orbit 16235) change in  
455 phase with the **ASYM/H AsyH** variations.

#### 4.3 Summary of the observations

Summarizing the results of Hall current observations by the CHAMP satellite during the magnetic disturbance period of 29–30 May 2003 in the daytime and nighttime sectors (12–16 MLT and 00–04 MLT, respectively) we conclude:

- 460 – Intense  $>1 \text{ A/m}$  eastward and westward electrojets can occur at latitudes of the auroral zone during substorm periods, which precede the magnetic storm, and during the beginning of its main phase. During the maximum of the main phase, the **density strength** of the Hall currents as well as the substorms diminish in antiphase to an increase of the **SYM/H SymH** index.
- 465 – A fast decay of the EE and WE occurs during the recovery phase at auroral latitudes both during daytime and nighttime hours. The westward or the eastward currents can be influenced during this storm phase by the existence of a PE at  $73^\circ < \text{MLat} < 80^\circ$  in the region of the dayside cusp.
- 470 – The direction of the current in the PE is determined by the IMF  $B_y$  component: for  $B_y > 0$  the current is eastward, for  $B_y < 0$  westward. The change of the current direction within the PE can occur several times during the storm development, but always in accordance with the change of the IMF  $B_y$  orientation.
- 475 – The Hall currents in the auroral ionosphere, both the EE and the WE, vary usually in phase with the **SYM/H SymH** and **ASYM/H AsyH** variations (but sometimes also in antiphase). There are time intervals, where any correlation between the geomagnetic activity indices and the Hall current parameters is missing. There is a closer connection of the current **density intensity** and the MLat variations with **ASYM/H AsyH** than with **SYM/H SymH**.
- In the daytime sector (14–16 MLT) during a period of intense substorms, the EE is located in a latitude range  $56^\circ < \text{MLat} < 64^\circ$ , while the WE is at  $64^\circ < \text{MLat} < 70^\circ$ . During the main phase

of the storm, the EE shifts to  $58^\circ < \text{MLat} < 62^\circ$ , while the WE is situated at  $64^\circ < \text{MLat} < 73^\circ$ , and during the recovery phase, finally, the WE is observed at latitudes of  $73^\circ < \text{MLat} < 76^\circ$ . Therefore, the EE stays at about the same latitudes during the both the intense substorms and the main phase of the storm, attaining extreme equatorward values of  $\text{MLat} \sim 56^\circ$ . An analogue situation exists with regard to the change of position for the WE in various storm phases, but during daytime hours the WE is located about  $6^\circ$  closer to the pole.

- In the nighttime sector (02–04 MLT), there exists practically only the WE, which is located during substorms at  $61^\circ < \text{MLat} < 64^\circ$ , and during the main storm phase at  $56^\circ < \text{MLat} < 60^\circ$ . Therefore, extremal positions of the WE and EE can reach latitudes below  $60^\circ$ . This occurs in the daytime sector for the EE, while in the nighttime for the WE.

The detailed description of the Hall current **dynamics characteristics** during five further magnetic summer storm intervals is transferred to the Appendix/**Supplementary material**.

## 5 **Discussion Correlation analyses and discussion**

In the section 4 and in the appendices A1–A5 we have investigated several geomagnetic storm periods, based on magnetometer measurements onboard the CHAMP satellite. The Hall currents in the high-latitude upper ionosphere of the Northern Hemisphere were analysed for various MLT sectors with regard to their position in geomagnetic latitude, their **density strength** and direction. The empirical description concerned the appearance of the EE, the WE, and the PE during various storm phases and was carried out primarily qualitatively.

Below we are going to analyse the current directions, their densities, and MLat positions for various MLT sectors with regard to solar wind parameters and some indices of the planetary magnetic activity (**SYM/H SymH**, **ASYM/H AsyH**, AL, IndN). We use activity indices, which characterize the occurrence and dynamics of large-scale plasma domains in Earth's magnetosphere that are responsible for the existence of concrete variations of the geomagnetic field at Earth's surface.

### 5.1 Polar electrojets

It is well-known from geomagnetic activity researches that the intense magnetic disturbances at the high-latitude projection of the magnetospheric cusp are not related to the occurrence and dynamics of magnetospheric substorms. ~~Wang et al., 2008, investigated the behaviour of electrojets by means of CHAMP satellite observations during two magnetic storm events with the focus on the auroral electrojets.~~ Fig. 3a–f shows **the correlations of the various IMF parameters and geomagnetic indices with the magnetic latitude (left side panels) and the Hall current density intensity  $I$  (right side panels)** obtained by CHAMP satellite crossings over the polar electrojets during 6 geomagnetic storms. The direction of the Hall currents can be distinguished in the upper panels (Fig. 3a): westward and

eastward currents are indicated with blue and red data points, respectively. For the further study, we selected the electrojet parameters at their extremal values of current **density strength** for each orbit. The data pool was augmented yet be including also neighbouring values before and after the  
515 extremal points.

**Table 2.** The dependent ( $X$ ) and independent variable ( $Y$ ), their correlation coefficients ( $r$ ), the coefficients  $A$  and  $B$  of the regression equations  $X = A + B * Y$ , and their dispersions  $\sigma$ .

X	Y	$r$	A	B	$\sigma$
I ( <b>density intensity</b> , A/m)	By (>0)	0.59	0.535	0.018	0.160
I ( <b>density intensity</b> , A/m)	By (<0)	-0.72	0.291	-0.024	0.134
I ( <b>density intensity</b> , A/m)	$ B_y $	0.56	0.433	0.018	0.170
I ( <b>density intensity</b> , A/m)	<b>ASYM/H AsyH</b>	0.74	0.396	0.004	0.138
MLat (deg)	AL	0.46	78.540	0.006	2.542
MLat (deg)	IndN	-0.52	77.750	-0.006	2.415

Fig. 3a differentiates the current measurements with regard to the azimuthal IMF component ( $B_y$ ), i.e., between those, obtained during  $B_y > 0$  and those during  $B_y < 0$  conditions. It is clearly seen that the direction of the current within the PE is determined by the IMF  $B_y$  sign. For intervals with positive IMF  $B_y > 0$ , we observe **for all cases** an eastward directed Hall current; for negative IMF  
520  $B_y < 0$  intervals the Hall current is always westward. The current **density strength** within the PE is correlated with the magnitude of the azimuthal IMF component  $B_y$ : it increases from 0.3–0.4 A/m for near-zero values to  $I \sim 0.9$  A/m for  $|B_y| \sim 23$  nT (i.e., the maximum  $B_y$  value during the periods **investigated-shown**). Correlation coefficients  $r$  between current **density intensity**  $I$  and the IMF  $B_y$  component for  $B_y > 0$  and  $B_y < 0$  are shown in the upper right and upper left corner, respectively  
525 (Fig. 3a, right panel). The coefficients for the offset ( $A$ ) and the slope ( $B$ ) of the linear regression line (for  $r \geq 0.46$ ) as well as the dispersion values  $\sigma$  are listed in Table 2.

The current **density intensity** values  $I$  for  $B_y \sim 0$  nT are somehow different in the regression equations for  $B_y > 0$  and  $B_y < 0$ . Fig. 3b (right panel) shows the current **density intensity**  $I$  as a function of the IMF component's magnitude  $|B_y|$ , i.e., independent of the IMF  $B_y$  sign. This  
530 increases the number of data points for linear regression estimation. According to this estimation, the current **density intensity** amounts to  $I \sim 0.4$  A/m for  $|B_y| \approx 0$  nT, while it attains  $\sim 0.9$  A/m for  $|B_y| = 23$  nT, i.e., about twice as large. The increase of the Hall current **density strength** within the PE **might take place during** can also occur in magnetically quiet intervals during the absence of magnetic activity at latitudes of the auroral zone, **which is because such disturbances are** not directly  
535 related to the IMF  $B_y$  component.

We could not find any essential correlation between the MLat position and the IMF  $B_y$  component for both  $B_y > 0$  ( $r = 0.04$ ) and  $B_y < 0$  ( $r = 0.32$ ) nor for  $|B_y|$  ( $r = 0.15$ , see Fig. 3a and b).

The current **density strength** and its direction (eastward or westward) within the PE is controlled by the IMF By component, but the latitudinal position of the current **density intensity** maximum does not depend on IMF By. The observed morphological peculiarity of the PE is caused by its generation mechanism. This is assumed to be due to the interaction between the magnetosphere and the supersonic plasma flow (solar wind) with a “frozen-in” magnetic field (IMF). The PE currents are generated at magnetic latitudes of the cusp due to reconnection processes between the IMF and the geomagnetic field (Jørgensen et al., 1972; Wilhelm and Friis-Christensen, 1971). The reconnection of magnetic fields brings about a north-south electric field and an east-west Hall current at cusp latitudes in the ionosphere. ~~A possible generation mechanism for the PE current system has been suggested by Leontyev and Lyatsky (1974), including the structure of the PE current system:~~

~~Leontyev and Lyatsky (1974) postulate the penetration of the electric field  $E_z = V_x \times B_y$ , where  $V_x$  is the solar wind velocity past the magnetosphere. This electric field will cause a potential difference  $U$  between the northern and southern boundaries of the magnetotail:  $U = E_z \times D_m$ , where  $D_m$  is the size of the magnetosphere along the z-axis. On the assumption of high conductivity along the magnetic field lines, the electric field  $E_z$  can exist only in the region of open field lines, rooted at the polar caps, and will be short-circuited along closed field lines. Thus, the boundary between closed and open field lines (OCB) will be the line of zero potential for the field  $E_z$ , and  $U=0$  at this boundary in the ionosphere.~~

~~Feldstein et al. (1975b) estimated the effectiveness of the electric field penetration from the solar wind to the cusp. During summer season (July–August 1969) the integral Hall current within the PE was estimated to  $\sim 220$  kA.~~

~~The integral conductivity in the ionosphere during summer around noon is  $\sim 7$  mhos, i.e., the potential drop in the cusp is about  $U \sim 30$  kV. The potential difference between the northern and southern boundaries of the magnetotail amount to  $U_m \sim 600$  kV.~~

~~The following assumptions were made for the estimation: solar wind speed  $V_x \sim 400$  km/s, IMF  $B_y = 6$  nT, and the magnetospheric size along the z-axis  $\sim 40 R_E$ .~~

~~If the voltage drop is the same in the northern and southern hemispheres, then the efficiency of the electric field penetration from the solar wind to the high-latitude ionosphere during summer season is  $\sim 10\%$ .~~

~~Here, we present estimations of the efficiency of the electric field penetration into the cusp region for two concrete orbits of the CHAMP satellite over the daytime sector.~~

~~During orbit 16238 of 30 May 2003 we observe a maximum Hall current density at 06:15 UT.~~

~~The solar wind velocity at this time was  $V_x = 640.7$  km/s, the plasma density in the solar wind  $n_p = 21.4 \text{ cm}^{-3}$ , and IMF  $B_y = 6$  nT. The electric field in the solar wind amounts to  $E_z = V_x \times B_y = 3.8$  mV/m. The dynamic plasma pressure at the subsolar point  $P_{sw} = 0.88 P_{sw}^{dyn} = 12.9$  nPa, while the distance of the subsolar point at the magnetopause is  $\sim 7 R_E$ .~~

~~The potential difference along the z-axis between the northern and southern tail boundaries~~

575 amounts to  $U_m = 338$  kV, and in the cusp of one hemisphere hence  $U_m = 169$  kV.

According to the CHAMP data, the mean density intensity of the current is  $\sim 0.3$  A/m over  $\sim 8.5^\circ$ ; the integral current in the cusp therefore  $\sim 295$  kA, and the potential difference in the cusp  $\sim 42$  kV. The efficiency of the electric field penetration from the solar wind into the ionosphere is thus about  $\sim 25\%$ .

580 During orbit 29018 of 24 Aug 2005, 16:42 UT, with  $V_x = 630.5$  km/s,  $n_p = 18.6$  cm $^{-3}$ , and IMF  $B_y = -20.9$  nT results in  $E_z = 12.6$  mV/m,  $P_{sw} = 10.8$  nPa, and distance of the subsolar point at the magnetopause is  $\sim 7.3 R_E$ . The potential difference in the cusp of one hemisphere can thus be estimated to  $U_m = 585$  kV. According to the CHAMP data, the mean density intensity of the current is  $\sim 0.4$  A/m over  $\sim 7.5^\circ$ , the integral current in the cusp therefore  $\sim 348$  kA, and the potential  
585 difference in the cusp  $\sim 49$  kV. The efficiency of the electric field penetration from the solar wind into the ionosphere is thus about  $\sim 9\%$ . Therefore, for a quite variable electric field voltage applied to the magnetosphere from the magnetized solar wind flow (from 585 kV to 169 kV), the efficiency of its penetration to the ionosphere varies between 9% and 25%.

The SYM/H SymH index varied during the intervals of CHAMP overflights above the polar elec-  
590 trojets considered in this study from -10 nT to -170 nT. As shown in Fig. 3c, there is no correlation between SYM/H SymH and the MLat positions ( $r = -0.13$ ) nor the PE current density strength ( $r = -0.01$ ). The absence of any correlation is as expected, because the current systems of the DCF, DR(sym), and DT are located completely within the magnetosphere. In case of absent FACs, they  
it cannot serve as a sources for Hall currents in the ionosphere that is responsible for the existence  
595 of PE.

According to Fig. 3d, there is a high correlation between the ASYM/H AsyH index and the PE current  $I$  ( $r \sim 0.74$ ) and an absence of correlation with the MLat position of the PE ( $r \sim -0.29$ ). The PE current density strength has therefore a direct relation to the intensity of the ASYM/H AsyH current system: with increasing longitudinal asymmetry increases the PE current density intensity,  
600 but the latitudinal position of the PE does not depend on ASYM/H AsyH.

A partial ring current (PRC) emerges during geomagnetic disturbances. The PRC is a westward directed current in the equatorial plane of the evening to nighttime sector at geocentric distances of  $R \sim 3-4 R_E$ . The basic PRC current system includes Region-2 FACs into the ionosphere within this sector (Iijima and Potemra, 1976a), and an EE in the ionosphere (Feldstein et al., 2006; Kalegaev  
605 et al., 2008). Observations of fluxes of energetic neutral atoms (ENA) show increased ion fluxes in the evening-nighttime sector within the inner magnetosphere during geomagnetic disturbances, which appears to be the experimental evidence for the existence of the PRC (Kozyreva and Liemohn, 2003). A successful modeling of the PRC and the EE has been performed by Kalegaev et al. (2008) for the magnetic storm event of November 06-14, 2004.

610 The high correlation between AsyH and the intensity of the PE gives reason to assume an IMF By control about the characteristics of the magnetic field asymmetry inside the magnetosphere. This

component of the IMF does not directly influence the intensity of the PRC, but via the current system, that forms by the PE with FACs between the PE and the PRC. The PRC position in the equatorial plane is controlled by MLT and toward the near noon sector it shifts to the ionospheric footpoint of the cusp region (Feldstein et al., 2006). The geocentric distance of the PRC increases therefore from the nighttime via the evening toward earlier hours. FACs of the PRC map from inner-magnetospheric heights to the near-cusp region, where the Hall currents flow, which are controlled by the IMF By component. In this way forms a PRC current system, which in addition to the basic one is controlled by the IMF By component.

Fig. 3e shows the correlation between the MLAT position and the ~~density strength~~ of the PE with the AL index of geomagnetic activity. ~~This index describes the reduction of the horizontal component of the geomagnetic field at auroral latitudes on Earth's surface during disturbances with respect to quiet-time conditions, using a longitudinal chain of magnetic observatories.~~ The AL index appears to be a sensitive tracer for processes in the central plasma sheet of the magnetospheric tail. These processes are created by injection of energetic particles, their accumulation, and the dissipation of their energy during storm times and is accompanied by changes of the boundary positions of large-scale plasma structures. They appear to have relatively small influence on the ~~density strength~~ and MLat position of the PE (with  $r = -0.38$  and  $r = 0.46$ , respectively). However, there is a distinctive tendency for the shift of the PE from  $\sim 78^\circ$  to  $\sim 74^\circ$  with an increase of the AL index up to  $-900$  nT.

As shown in Fig. 3f, there is a correlation of IndN with MLat in the daytime sector ( $r=-0.52$ ). This is obvious, because both components By and Bz are included in the definition of IndN. With increasing IndN, the latitude of the current decreases. The correlation coefficient of IndN with the Hall current ~~density intensity~~ ( $I$ ) is  $r=0.3$ .

To summarize, the values of the correlation coefficients  $r$  and the coefficients  $A$  and  $B$  of the regression equations are listed in Table 2. They relate the PE current intensity and their MLat position to the indices that characterize the situation in the solar wind and within the magnetosphere at the time of the observations. The PE are characterized by the following peculiarities:

- The PE appears at magnetic latitudes and local times of the cusp.
- The direction of the current in the PE is controlled by the IMF By (azimuthal) component: for  $B_y > 0$  the current is eastward, for  $B_y < 0$  the current is westward directed.
- The current strength in the PE increases with the intensity of the IMF By component from  $I \sim 0.4$  A/m for  $B_y \sim 0$  nT up to  $I \sim 1.0$  A/m for  $B_y \sim 23$  nT.
- The MLat position of the PE does not depend on the orientation and the strength of the IMF By component.

- There is no connection between MLat and the current intensity  $I$  in the PE with the magnetospheric ring current DR (index SymH).
- There is a correlation between the current intensity  $I$  in the PE and the strength of the partial ring current in the magnetosphere (PRC, index AsyH), but practically no correlation of this index with MLat of the PE.
- The currents in the central plasma sheet appear to have a weak influence on the current intensity and the MLat position of the cusp.
- We realized a correlation between MLat and the IndN solar wind coupling function.

## 5.2 Auroral electrojets

The most intense Hall currents at ionospheric heights, which are responsible for the electrojets, are located at auroral latitudes in the nighttime hours. It is even there, where intense auroras occur most often in the zenith (Chapman and Bartels, 1940; Harang, 1951). These electrojets were named auroral electrojets (AE). A huge number of studies has been published on their morphology, their connections with the solar wind parameters and the plasma domains in Earth's magnetosphere, as well as on their internal processes. The AE are present during all hours of the day. Based on magnetometer data of the IMAGE and EISCAT networks, Feldstein et al. (1997) showed that the electrojets shift equatorward during the main phase of strong magnetic storms. For  $DST \sim -300$  nT, the EE in the evening and the WE in the nighttime and early morning hours shifts to  $\sim 54^\circ$ – $\sim 55^\circ$ . The number of electrojets, their internal current structure, and the interconnection with the individual magnetospheric plasma domains depends both on the activity level and on the MLT position of the observation (Feldstein et al., 2006). Therefore, we consider below the results of the Hall current observations of the CHAMP satellite separately for each of the following four MLT sectors: daytime, nighttime, evening, and morning hours.

Figures 4–7 consider the MLat positions (left columns) and current densities  $I$  (right columns) during the moments of extreme values of current density strength in dependence on the SYM/H SymH, ASYM/H AsyH, AL, and IndN indices. As in Fig. 3a, data points of electrojets with an eastward direction are indicated by red colour and those with westward direction by blue colour.

Table 3 provides the correlation coefficients  $r$ , the coefficients  $A$  and  $B$  of the linear regression equations of the type  $X = A + B * Y$ , which were obtained by the least-squares method with correlation coefficients  $r > 0.46$ , and the mean-square deviation  $\sigma$  from the regression line.

### 5.2.1 Daytime sector 09:00–14:00 MLT

The AE in the daytime sector can coexist with the PE. These two types of current can be distinguished according to the following indications (that are valid for AE in contrast to PE):



**Table 3.** The dependent ( $X$ ) and the independent variable ( $Y$ ), their correlation coefficients ( $r$ ), the coefficients  $A$  and  $B$  of the regression equations  $X = A + B * Y$ , and their dispersions  $\sigma$ , listed for four different MLT intervals.

X	Y	$r$	A	B	$\sigma$
<b>MLT 09:00–13:594:00</b>					
MLat (WE, deg)	ASYM/H AsyH	-0.54	74.136	-0.052	3.89
MLat (EE, deg)	ASYM/H AsyH	-0.49	70.327	-0.047	3.91
MLat (EE, deg)	AL	0.68	70.192	0.005	3.28
MLat (WE, deg)	IndN	-0.74	72.215	-0.011	3.13
MLat (EE, deg)	IndN	-0.67	70.271	-0.025	3.43
<b>MLT 14:00–20:591:00</b>					
MLat (WE, deg)	SYM/H SymH	0.49	72.783	0.041	4.23
MLat (EE, deg)	ASYM/H AsyH	-0.54	65.971	-0.036	3.67
Intensity (WE, A/m)	ASYM/H AsyH	0.68	0.168	0.003	0.24
Intensity (EE, A/m)	ASYM/H AsyH	0.64	0.217	0.004	0.29
MLat (EE, deg)	AL	0.46	64.707	0.004	3.88
Intensity (EE, A/m)	AL	-0.59	0.320	-0.001	0.31
<b>MLT 21:00–01:592:00</b>					
MLat (WE, deg)	SYM/H SymH	0.53	63.806	0.032	2.25
Intensity (WE, A/m)	ASYM/H AsyH	0.50	0.205	0.005	0.33
Intensity (WE, A/m)	AL	-0.67	0.233	-0.001	0.28
Intensity (WE, A/m)	IndN	0.76	0.207	0.003	0.25
<b>MLT 02:00–08:599:00</b>					
MLat (WE, deg)	SYM/H SymH	0.47	67.343	0.040	3.24
Intensity (WE, A/m)	ASYM/H AsyH	0.69	-0.089	0.010	0.38
Intensity (WE, A/m)	AL	-0.52	0.328	-0.001	0.44

1. The AE are as a rule located at MLat<73° during low geomagnetic activity conditions;

680 2. the Hall current direction in the AE does not depend uniquely from the orientation of the IMF  
By component.

Fig. 4a shows ~~only those~~ cases of AE appearance in the daytime sector with ~~changing a change~~  
of the SYM/H SymH index. Usually, SYM/H SymH has negative values (SYM/H SymH<0 nT)  
during geomagnetic storms. Fig. 4a shows, however, beside of the mostly negative values also some  
685 values with SYM/H SymH>0. They occur as a rule during the first few hours of magnetic storms.

The large scatter of the data points and their low correlation coefficients (maximum for MLat(EE,  $r = 0.39$ ) and  $I(\text{EE}, r = 0.29)$  in Fig. 4a) indicate the weak control of the AE parameters by the symmetric ring current, the index of which is **SYM/H SymH**.

The MLat position of the AE in the daytime sector correlates with three other indices: **ASYM/H**  
 690 **AsyH**, AL, and IndN. The AE shifts with increasing disturbances toward lower latitudes: the WE from  $72^\circ$  to  $66^\circ$ , and the EE from  $70^\circ$  to  $57^\circ$  (Fig. 4b–d). The largest correlations of MLat are found with the IndN coupling function (WE,  $r = -0.74$ ), the smallest values for **ASYM/H AsyH** (EE,  $r = -0.49$ ). **IndN is proportional to the amount of opened magnetic flux per unit time in the polar cap, which in turn affects the current systems.**

695 These ~~three~~ **AL and AsyH** indices characterize the large-scale current systems, the magnetic fields of which influence the magnetic field configuration of the dayside sector. It should be noted that there are tendencies for the WE to be located during daytime hours a few degrees more poleward than the EE. These tendencies are clearly visible with regard to the MLat(EE and WE) positions and their relation to **ASYM/H AsyH** and IndN (Fig. 4b and d). The constant term  $A$  is in the case of **ASYM/H**  
 700 **AsyH**  $3.8^\circ$  larger for the WE than for the EE, and  $1.9^\circ$  in the case of the solar wind coupling function IndN.

The correlation coefficients for the Hall current with the IMF  $B_y$  vector component and its magnitude is low (not shown). A significant correlation coefficient  $|r| > 0.49$  is achieved in the daytime sector only for the MLat positions of the electrojets, while the correlation with the current densities is minimal **for all indices**. The electrojets can be both westward and eastward. The EE can be  
 705 observed for very intense disturbances during the storm period down to  $\text{MLat} \sim 57^\circ$ .

### 5.2.2 Evening sector 14:00–21:00 MLT

**Figure 5 provides data presentations in the same format as Fig. 4, but now for the evening sector.** Significant correlation values  $r$  exist in the evening sector for both the current densities and the MLat  
 710 positions of the electrojets. The largest values of  $r \sim 0.6 - 0.7$  were obtained for current densities  $I$ , independent of the current directions (westward or eastward) in the electrojets.

There appears a dependence of MLat(WE) from the **SYM/H SymH** index: the electrojets shifts equatorward with an increase of the ring current. The EE is located more equatorward than the WE by about  $\sim 6^\circ$ . The constant term  $A$  of the regression equations amounts accordingly to  $\text{MLat}(\text{EE}) \sim 66^\circ$   
 715 with respect to **ASYM/H AsyH** and  $\text{MLat}(\text{WE}) \sim 72^\circ$  with respect to **SYM/H SymH**.

The EE current **density strength** exceeds those of the WE. That means, the interpretation of the EE in the evening sector as a branch-off from the WE at higher latitudes will become more unlikely  
 (Feldstein et al., 2006).

The electrojets move more equatorward with increasing disturbance level according to any geo-  
 720 magnetic activity index. Their current densities rise from  $<0.2$  A/m to 1.6 A/m for the EE, and up to 1.3 A/m for the WE. **The current strength of the EE increases hence stronger than that of the WE**

(by about 30%). The EE is observed equatorward of MLat $\sim$ 60° during magnetic storm periods with the threshold latitude for the EE shift of  $\sim$ 53°.

### 5.2.3 Midnight sector 21:00–02:00 MLT

725 In this sector, the WE exists almost exclusively (Fig. 6). Moreover, the current ~~density intensity~~ correlates here well with the ~~ASYM/H~~ AsyH, AL, and IndN indices with a maximum value of  $r = 0.76$  for the IndN coupling function.

~~Otherwise, †~~ The MLat(WE) position, ~~however~~, correlates only with the ~~SYM/H~~ SymH index. It decreases from 62° to 58° for a change of ~~SYM/H~~ SymH from  $\sim$ -40 nT to  $\sim$ -170 nT. ~~The lowest~~  
730 ~~possible MLat appears to be  $\sim$ 58°.~~

The WE current ~~density strength~~ increases from values  $<0.2$  A/m to  $\sim 1.5$  A/m for an intensification of the disturbance according to the IndN coupling function from 0 to 325, while the WE position ~~moves equatorward until a may have an equatorward~~ threshold value of  $\sim 58^\circ$ .

### 5.2.4 Morning sector 02:00–09:00 MLT

735 Similar to the midnight sector, the WE exists also almost exclusively within the morning sector (Fig. 7). The current ~~density intensity~~ correlates here well with the ~~ASYM/H~~ AsyH and AL, with a maximum value of  $r = 0.69$  for the ~~ASYM/H~~ AsyH index. The WE current ~~density strength~~ increases from values 0.32 A/m to 1.92 A/m with an increase of the ~~ASYM/H~~ AsyH value from 40 nT to 200 nT, while the electrojet position moves equatorward until a threshold value of  $\sim 56^\circ$ .

740 The MLat(WE) position correlates only with the ~~SYM/H~~ SymH index. In this regard the midnight and morning sectors show the same behaviour. The MLat positions are controlled predominantly by the ~~SYM/H~~ SymH index, i.e., by the ~~density intensity~~ of the ring current DR rather than by any other current system.

The central plasma sheet of the magnetospheric tail is the source region of the WE in the nighttime  
745 sector. An increase of the DR is accompanied by a change of the geometry of the magnetic field lines that are interconnected with the central plasma sheet. This results in a shift of the ionospheric projection of the WE toward the equator. The relation between the current ~~density intensity~~ in the WE and the AL value is not needed for the interpretation.

## 6 Conclusions

750 In this paper we investigated the ~~density strength~~ and spatial-temporal distribution (versus magnetic latitude MLat and MLT) of Hall currents at high latitudes. The currents were determined from measurements of ~~total scalar~~ magnetic field data, sampled ~~by magnetometers~~ on board the CHAMP satellite at ionospheric altitudes of  $\sim 430$  km (Ritter et al., 2004a) ~~—In this study we used these current estimations to explore the dynamics characteristics of the polar and auroral electrojets during~~

a selection of six magnetic storms (see Table 1). ~~We identified their distinctive features and the correlations with activity indices that are usually used to characterize large-scale current systems in the magnetosphere.~~ The main findings obtained are ~~listed below~~ as follows.

The current intensity of the PE increases with the magnitude of the IMF By component, while no correlation at all could be found between the MLat position of the PE and the IMF By component.

The PE is eastward directed for IMF By>0 and westward for IMF By<0. Changes of current flow direction in the PE can occur manifold during the storm, but only due to changes of the IMF By orientation. There is a strong correlation between the PE current strength and the extent of the ring current asymmetry as indicated by the AsyH index, while there is no connection with the SymH index, the symmetric part of the ring current. There is an IMF By control of the magnetic field asymmetry inside the magnetosphere that manifests in the high correlation between AsyH and the PE current intensity.

Auroral electrojets are located at auroral latitudes (MLat<72° during daytime hours, and MLat<68° during nighttime) and exist during all MLT. The number of electrojets in a certain latitude range, the structure of the currents in them, and the interconnection with concrete magnetospheric plasma domains, depend on the disturbance level, which is controlled by UT as well as local time (MLT) at the observational points. Around midnight, the WE is predominant, and it exists almost exclusively in the morning sector. During daytime hours, the MLat positions of the auroral electrojets, both WE and EE, correlate with the activity indices AsyH, AL, and IndN. The correlation with the current intensities, however, is relatively small there for all indices. The largest correlations ( $r \sim 0.6-0.7$ ) exist between the AsyH index and the current intensity of the electrojets in the evening sector.

Certain characteristic features of the electrojets appear during the different phases of a geomagnetic storm. With the development of the main phase both the daytime EE and the nighttime WE shift to subauroral latitudes MLat~56°, while increasing in strength up to  $I \sim 1.5$  A/m. During evening hours, the WE is located by ~6° closer to the pole than the EE. A splitting of the WE is possible in the morning hours during the recovery phase, analogous to the splitting of auroral luminescence in the auroral oval.

The EE displaces in the region of diffuse aurora, equatorward of the discrete auroral forms, and projects along magnetic field lines into the inner magnetosphere between the plasmasphere and the central plasma sheet of the magnetospheric tail (Galperin and Feldstein, 1996).

## 6.1 Variations of the Hall currents during storms

- ~~The characteristics and density intensity of Hall currents change in the course of geomagnetic storms. Their structure correspond basically to the well-known characteristics and dynamics of electrojets in MLat and MLT during magnetic storms. A splitting of the WE is possible in the morning hours during the recovery phase, analogous to the splitting of auroral luminescence in the auroral oval. These are additional, though indirect affirmations for the applicability to~~

use magnetic field measurements at altitudes above the main ionospheric current layer for the determination of currents in the upper ionosphere.

- Substorms occurring prior to or during the beginning of the main phase of a storm are accompanied by an EE at auroral latitudes ( $MLat \sim 64^\circ$ ) during daytime MLT hours. Later they appear as WE both in the afternoon ( $64^\circ < MLat < 70^\circ$ ) and during nighttime ( $MLat \sim 64^\circ$ ).
- With the development of the main phase both the daytime EE and the nighttime WE shift to subauroral latitudes  $MLat \sim 56^\circ$ , while increasing in density strength up to  $I \sim 1.5$  A/m. Both electrojets exist during daytime and evening hours in the main storm phase. During evening hours, the WE is located by  $\sim 6^\circ$  closer to the pole than the EE, and about  $2^\circ$ – $3^\circ$  during daytime hours.
- The current densities of EE and WE decrease quickly during the recovery phase, i.e., the electrojets vanish, but in the daytime sector at  $MLat \sim 73^\circ$ – $80^\circ$  appears a PE (polar electrojet) with a westward or an eastward direction, depending on the orientation of the IMF  $B_y$  component. The PE is eastward directed for  $B_y > 0$  and westward directed for  $B_y < 0$ . Changes of current flow direction in the PE can occur manifold during the storm, but only due to changes of the IMF  $B_y$  orientation.

## 6.2 Hall current in the polar electrojet

While auroral electrojets are present at all local time hours, the PE is confined to daytime hours. Fig. 3a–f shows the results of the correlation analysis of the PE characteristics and the IMF  $B_y$  component as well as various activity indices. The values of the correlation coefficients  $r$  and the coefficients  $A$  and  $B$  of the regression equations are listed in Table 2. They relate the current density intensity and their  $MLat$  position to the indices that characterize the situation in the solar wind and within the magnetosphere at the time of the observations.

The PE currents and their  $MLat$  positions are characterized by the following peculiarities:

- The PE appears at magnetic latitudes and local times of the cusp.
- The direction of the current in the PE is controlled by the IMF  $B_y$  (azimuthal) component: for  $B_y > 0$  the current is eastward, for  $B_y < 0$  the current is westward directed.
- The current density strength in the PE increases with the intensity of the IMF  $B_y$  component from  $I \sim 0.4$  A/m for  $B_y \sim 0$  nT up to  $I \sim 1.0$  A/m for  $B_y \sim 23$  nT.
- The  $MLat$  position of the PE does not depend on the orientation and the strength of the IMF  $B_y$  component.

- Assuming that the penetration of the solar wind electric field into the cusp causes the generation of the PE, we estimate the efficiency of such a penetration. Based on two CHAMP orbits across the dayside sector of the high-latitude ionosphere, we estimate the potential difference over the cusp with 169 kV and 585 kV. The efficiency of the electric field penetration into the cusp would then amount to 25% and 9%, respectively.
- There is no connection between MLat and the current density intensity  $I$  in the PE with the magnetospheric ring current DR (index SYM/H SymH).
- There is a correlation between the current density intensity  $I$  in the PE and the density strength of the partial ring current in the magnetosphere (PRC, index ASYM/H AsyH), but practically no correlation of this index with MLat of the PE.
- The currents in the central plasma sheet appear to have a weak influence on the current density intensity and the MLat position of the cusp.
- We realized a correlation between MLat and the IndN solar wind coupling function.

### 6.3 Hall current in auroral electrojets

Auroral electrojets are located at auroral latitudes (MLat  $< 72^\circ$  during daytime hours, and MLat  $< 68^\circ$  during nighttime) exist during all MLT. The amount of electrojet current in a certain latitude range, the structure of the currents in them, the interconnection with concrete magnetospheric domains, depends on the level of disturbance, which is controlled by UT as well as local time (MLT) at the observational points. Therefore we present the conclusions from the observations for each of the four time sectors: daytime, evening, nighttime, and morning hours.

Daytime sector (09–14 MLT):

- The MLat positions of the auroral electrojets, both WE and EE, correlate with the activity indices ASYM/H AsyH, AL, and IndN. The auroral electrojets shift toward lower latitudes with increasing activity. For ASYM/H AsyH  $\sim 220$  nT the EE shifts to MLAT  $\sim 57^\circ$ .
- MLat(EE) collocates  $3.8^\circ$  equatorward of MLat(WE) according to the ASYM/H AsyH index and  $1.9^\circ$  according to the IndN coupling function.
- Significant correlation coefficients with  $r > 0.49$  are obtained only for MLat, correlations with the current density intensity  $I$  are, however, very small for all indices.

Evening sector (14–21 MLT):

- Significant values of the correlation coefficients  $r$  with activity indices exist both for MLat and for the Hall current density intensity  $I$ .

- The largest correlation coefficients ( $r \sim 0.6-0.7$ ) exist between the ASYM/H AsyH index and the current density intensity  $I(\text{WE}, \text{EE})$ .

855

- The EE shifts  $\sim 6^\circ$  more equatorward compared to the WE.
- The EE and WE shift equatorward with increasing activity. This shift occurs with respect to all activity indices inspected here. The EE is located equatorward of MLat  $\sim 60^\circ$  during magnetic storm periods; the farthest shift attains MLat  $\sim 53^\circ$ .

860

- The equatorward shift for increasing activity is accompanied by increasing current densities from  $I < 0.2 \text{ A/m}$  for ASYM/H AsyH  $\sim 40 \text{ nT}$  to  $\sim 1.7 \text{ A/m}$  in the EE and  $\sim 1.3 \text{ A/m}$  in the WE for ASYM/H AsyH  $\sim 380 \text{ nT}$ . The current density strength of the EE increases hence stronger than that of the WE (by about 30%).

865

- The current density strength in the EE is larger than in the WE. The WE is missing for a certain confined MLT interval of the evening sector, in case of an existing EE (Feldstein et al., 2006). That means that the EE in the evening sector cannot be a low-latitude branch-off from the WE current.

Near-midnight sector (21–02 MLT):

- Around midnight, the WE is predominant.
- The current density strength in the WE correlates with the activity indices ASYM/H AsyH, AL, and IndN, with a maximum correlation coefficient of  $r \sim 0.76$  for the IndN.
- The MLat(WE) position correlates only with the SYM/H SymH index, shifting equatorward from  $62^\circ$  to  $58^\circ$  for a SYM/H SymH increase from  $-40 \text{ nT}$  to  $-170 \text{ nT}$ . The lowest possible MLat is  $\sim 58^\circ$ .

870

- The equatorward shift of the WE is accompanied by an increase of the current density intensity from  $I < 0.2 \text{ A/m}$  to  $\sim 1.5 \text{ A/m}$ .

875

Morning sector (02–09 MLT):

The characteristics of the auroral electrojets is almost identical for midnight and morning hours.

- The MLat position at that MLT is controlled for the most part by the SYM/H SymH activity index, i.e., by the density strength of the ring current.
- In the morning sector, there exists almost exclusively the WE only.
- The current density intensity in the WE correlates with the ASYM/H AsyH and the AL indices with maximum values of  $r = 0.69$  with respect to ASYM/H AsyH.
- The current density strength increases from  $0.5 \text{ A/m}$  to  $2.1 \text{ A/m}$  for intensifications of ASYM/H AsyH from  $40 \text{ nT}$  to  $200 \text{ nT}$ .

880



885       – With increasing activity, the WE shifts equatorward. The lowest observed MLat for the WE is  
           $\sim 58^\circ$ .

The existing morphological differences between the EE and the WE probably testify differences  
of the physical sources, which are responsible for the existence of the EE and WE. One possible  
option is the interpretation of the EE in the evening and daytime sectors as continuation of the  
890 magnetospheric partial ring current (PRC) through the ionosphere via a system of FACs. The  
WE, which is situated  $\sim 6^\circ$  poleward of the EE in the evening sector, might be the ionospheric  
continuation of the WE in the evening hours, which is connected via FACs with the central plasma  
sheet in the magnetospheric tail in the nighttime and morning sectors.

*Acknowledgements.* The compilation of the storms and the corresponding IMF conditions during the inter-  
vals selected was conducted by use of the one-minute OMNI data base (<http://omniweb.gsfc.nasa.gov/>). The  
895 CHAMP mission was sponsored by the Space Agency of the German Aerospace Center (DLR) through funds  
of the Federal Ministry of Economics and Technology, following a decision of the German Federal Parlia-  
ment (grant code 50EE0944). The data retrieval and operation of the CHAMP satellite by the German Space  
Operations Center (GSOC) of DLR is acknowledged.

## 900 References

- ~~Alexeev, I. I., Belenkaya, E. S., Kalegaev, V. V., Feldstein, Y. I., and Grafe, A.: Magnetic storms and magnetotail currents, *J. Geophys. Res.*, 101, 7737–7747, 1996.~~
- Baumjohann, W. and Treumann, R. A.: Basic Space Plasma Physics, Imperial College Press, London, 1996.
- Chapman, S.: The electric current systems of magnetic storms, *Terr. Magn. Atmos. Elect.*, 40, 349–370, 1935.
- 905 Chapman, S. and Bartels, J.: *Geomagnetism, 1, Geomagnetic and related phenomena*, Clarendon Press, Oxford, 542p., 1940.
- Cowley, S. W. H.: *Dungey's Reconnection Model of the Earth's Magnetosphere: The first 40 Years*, vol. 41 of *Astrophysics and Space Science Proceedings*, pp. 1–32, Springer International Publishing, Switzerland, doi:10.1007/978-3-319-18359-6\_1, 2015.
- 910 Cowley, S. W. H. and Lockwood, M.: Excitation and decay of solar wind-driven flows in the magnetosphere-ionosphere system, *Ann. Geophys.*, 10, 103–115, 1992.
- Dungey, J. W.: Interplanetary magnetic field and the auroral zones, *Phys. Rev. Lett.*, 6, 47–48, 1961.
- Elphinstone, R. D., Murphree, J. S., and Cogger, L. L.: What is a global auroral substorm?, *Rev. Geophys.*, 34, 169–232, 1996.
- 915 Feldstein, Y. I.: Magnetic field variations in the polar region during magnetically quiet periods and interplanetary magnetic fields, *Space Sci. Rev.*, 18, 777–861, 1976.
- Feldstein, Y. I. and Levitin, A. E.: Solar wind control of electric fields and currents in the ionosphere, *J. Geomag. Geoelectr.*, 38, 1143–1182, 1986.
- Feldstein, Y. I., Lyatskaya, A. M., Sumaruk, P. V., and Shevnina, N. F.: Ionisation of the E-layer and the
- 920 variations of the magnetic field in the near-polar region (in Russian), *Geomagn. Aeron.*, 15, 1021–1027, 1975a.
- Feldstein, Y. I., Sumaruk, P., and Shevnina, N. F.: To the diagnostics of the azimuthal component of the interplanetary magnetic field, *C. R. Acad. Sci. USSR*, 222, 833–836, 1975b.
- Feldstein, Y. I., Grafe, A., Gromova, L. I., and Popov, V. A.: Auroral electrojets during geomagnetic storms, *J.*
- 925 *Geophys. Res.*, 102, 14,223–14,235, doi:10.1029/97JA00577, 1997.
- Feldstein, Y. I., Popov, V. A., Cumnock, J. A., Prigancova, A., Blomberg, L. G., Kozyra, J. U., Tsurutani, B. T., Gromova, L. I., and Levitin, A. E.: Auroral electrojets and boundaries of plasma domains in the magnetosphere during magnetically disturbed intervals, *Ann. Geophys.*, 24, 2243–2276, 2006.
- Friis-Christensen, E. and Wilhelm, J.: Polar currents for different directions of the interplanetary magnetic
- 930 field in the Y - Z plane, *J. Geophys. Res.*, 80, 1248–1260, 1975.
- Friis-Christensen, E., Laasen, K., Wilhelm, J., Wilcox, J. M., Gonzales, W., and Colburn, D. S.: Critical Component of the Interplanetary Magnetic Field Responsible for Large Geomagnetic Effects in the Polar Cap, *J. Geophys. Res.*, 77, 3371–3376, 1972.
- Friis-Christensen, E., Kamide, Y., Richmond, A. D., and Matsushita, S.: Interplanetary magnetic field control
- 935 of high-latitude electric fields and currents determined from Greenland magnetometer data, *J. Geophys. Res.*, 90, 1325–1338, 1985.
- Fukushima, N.: Generalized theorem for no ground magnetic effect of vertical currents connected with Pedersen currents in the uniform-conductivity ionosphere, *Rep. Ionosph. Space Res. Jap.*, 30, 35–40, 1976.
- Galperin, Y. I. and Feldstein, Y. I.: Mapping of the precipitation regions to the plasma sheet, *J. Geomag.*

- 940     Geoelectr., 48, 857–875, 1996.
- Green, D. L., Waters, C. L., Korth, H., Anderson, B. J., Ridley, A. J., and Barnes, R. J.: Technique: Large-scale ionospheric conductance estimated from combined satellite and ground-based electromagnetic data, *J. Geophys. Res.*, 112, doi:10.1029/2006JA012069, 2007.
- Harang, L.: *The Aurorae*, vol. 1, Chapman & Hall, Ltd., London, The International Astrophysical Series edn.,  
945     163p., 1951.
- Iijima, T. and Potemra, T. A.: The amplitude distribution of the field-aligned currents at northern high latitudes observed by TRIAD, *J. Geophys. Res.*, 81, 2165–2174, 1976a.
- Iijima, T. and Potemra, T. A.: Field-aligned currents in the dayside cusp observed by TRIAD, *J. Geophys. Res.*, 81, 5971–5979, 1976b.
- 950     Iijima, T., Potemra, T. A., Zanetti, L. J., and Bythrow, P. F.: Large-scale Birkeland currents in the dayside polar region during strongly northward IMF: A new Birkeland current system, *J. Geophys. Res.*, 89, 7441–7452, 1984.
- Jørgensen, T. S., Friis-Christensen, E., and Wilhelm, J.: Interplanetary magnetic-field direction and high-latitude ionospheric currents, *J. Geophys. Res.*, 77, 1976–1977, doi:10.1029/JA077i010p01976, 1972.
- 955     Kalegaev, V. V., Bakhmina, K. V., Alexeev, I. I., Belenkaya, E. S., Feldstein, Y. I., and Ganushkina, N. Y.: Asymmetry of the ring current during geomagnetic disturbances, *Geomagn. Aeron. (Engl. translation)*, 48, 780–792, 2008.
- Kozyreva, J. U. and Liemohn, M. W.: Ring current energy input and decay, *Space Sci. Rev.*, 109, 105–131, 2003.
- 960     Laundal, K. M., Finlay, C. C., Olsen, N., and Reistad, J. P.: Solar Wind and Seasonal Influence on Ionospheric Currents From Swarm and CHAMP Measurements, *J. Geophys. Res.*, doi:10.1029/2018JA025387, 2018.
- ~~Leontyev, S. V. and Lyatsky, W. B.: Electric field and currents connected with Y-component of interplanetary magnetic field, *Planet. Space Sci.*, 22, 811–819, 1974.~~
- Levitin, A. E., Afonina, R. G., Belov, B. A., and Feldstein, Y. I.: Geomagnetic variations and field-aligned  
965     currents at northern high-latitudes and their relations to solar wind parameters, *Philos. Trans. Royal Soc., A304*, 253–301, 1982.
- ~~Maltsev, Y. P.: Points of controversy in the study of magnetic storms, *Space Sci. Rev.*, 110, 227–267, 2004.~~
- Mansurov, S. M.: New evidence of the relationship between magnetic field in space and on the Earth, *Geomagn. Aeron. (Engl. translation)*, 9, 768–773, 1969.
- 970     Milan, S. E.: Sun et Lumière: Solar wind-magnetosphere coupling as deduced from ionospheric flows and polar auroras, vol. 41 of *Astrophysics and Space Science Proceedings*, pp. 33–64, Springer International Publishing, Switzerland, doi:10.1007/978-3-319-18359-6\_2, 2015.
- Newell, P. T., Sotirelis, T., Liou, K., Meng, C.-I., and Rich, F. J.: A nearly universal solar wind-magnetosphere coupling function inferred from 10 magnetospheric state variables, *J. Geophys. Res.*, 112, A01206, doi:  
975     10.1029/2006JA012015, 2007.
- Olsen, N.: A new tool for determining ionospheric current from magnetic satellite data, *Geophys. Res. Lett.*, 23, 3635–3638, 1996.
- Reigber, C., Lühr, H., and Schwintzer, P.: CHAMP mission status, *Adv. Space Res.*, 30, 129–134, 2002.
- Richmond, A. D.: Ionospheric electrodynamics using magnetic Apex coordinates, *J. Geomag. Geoelectr.*, 47,

- 980     191–208, 1995.
- Ritter, P., Lühr, H., Maus, S., and Viljanen, A.: High-latitude ionospheric currents during very quiet times: their characteristics and predictability, *Ann. Geophys.*, 22, 2001–2014, 2004a.
- Ritter, P., Lühr, H., Viljanen, A., Amm, O., Pulkkinen, A., and Sillanpää, I.: Ionospheric currents estimated simultaneously from CHAMP satellite and IMAGE ground-based magnetic field measurements: a statistical  
985     study at auroral latitudes, *Ann. Geophys.*, 22, 417–430, 2004b.
- Sandholt, P. E., Carlson, C., and Egeland, A.: Dayside and polar cap aurora, vol. 270 of *Astrophys. Space Sci. Library*, Kluwer Academ. Pub., Dordrecht/Boston/London, 287p., 2002.
- Sandholt, P. E., Farrugia, C. J., and Denig, W. F.: Detailed day-side auroral morphology as a function of local time for southern IMF orientation: implications for solar wind-magnetosphere coupling, *Ann. Geophys.*, 22,  
990     3537–3560, 2004.
- Sumaruk, P. V. and Feldstein, Y. I.: Sector structure of the interplanetary magnetic field and the magnetic variations in the near-polar region (in Russian), *Kosm. Issled.*, 11, 155–160, 1973.
- Svalgaard, L.: Sector structure of the interplanetary magnetic field and daily variation of the geomagnetic field at high latitudes, in: *Geophys. Papers, R-6*, Danish Meteorol. Inst., 1968.
- 995     Wang, H., Lühr, H., Ridley, A., Ritter, P., and Yu, Y.: Storm time dynamics of auroral electrojets: CHAMP observation and the Space Weather Modeling Framework comparison, *Ann. Geophys.*, 26, 555–570, 2008.
- Wilhelm, J. and Friis-Christensen, E.: Electric field and high latitude zonal currents induced by merging of field lines, in: *Geophys. Paper R-31*, Dan. Meteorol. Inst., Charlottenlund, Denmark, 1971.

## Appendix A Detailed description of the dynamics of further storm intervals

1000 A1 The magnetic storm of 24 August 2005

This storm began with a sudden storm commencement (SSC) at 06:15 UT, which appeared as a jump-like increase of the **SYM/H SymH** index up to  $\sim 30$  nT. The storm phases were identified according to the 1-min values of the **SYM/H SymH** index. Fig. A1.1 shows the magnetic activity indices **SYM/H SymH**, **ASYM/H AsyH**, AU, AL, and the IMF components By and Bz.

1005 The orbits 29012 and 29013 take place during the **ereation growth** phase of the storm, the orbits 29014 and 29015 during the main phase, and the orbits 29016–29020 during the recovery phase. The direction and **density strength** of the Hall currents along the orbits are shown in Fig. A1.2 during daytime hours on the left hand side corresponding to the ascending orbital sections, and on the right hand side during nighttime hours for descending orbital sections. The crossings of the auroral oval  
1010 occurs between 12–13 MLT during daytime and 23–24 MLT for the nighttime column. Positive values denote an eastward current (EE) for the descending orbits, and a westward current (WE) for the ascending orbital sections.

The index values during the **ereation growth** phase of the storm are in the range of 25.5–32.7 nT for **SYM/H SymH**, 121.1–72.0 nT for **ASYM/H AsyH**, while the substorms achieve  $\sim 1000$  nT  
1015 according to the AL index. **SYM/H SymH** intensifies during the main phase up to -155.6 nT and **ASYM/H AsyH** to 206.6 nT, where intense substorms with AL  $\sim 3000$  nT occur. **ASYM/H AsyH** values decrease to 43.5 nT during the recovery phase, and we observe weakly variable **SYM/H SymH** index values around -120 nT (see Fig. A1.1).

An EE exists during daytime hours of orbit 29012 with a current **density intensity** of up to  
1020 1.37 A/m at MLat 72.6°. During the subsequent orbit, the eastward current **density intensity** diminishes to 0.44 A/m at MLat 70.3°. The intensification of **SYM/H SymH** during the main storm phase (orbit 29015) is accompanied by a continuing decrease of the eastward Hall current to 0.38 A/m at MLat=65.4°. An EE with a **density strength** of  $\sim 0.7$  A/m around midday is recorded at MLat=57.3°, i.e., below 60°, only in connection with very intense substorms (Fig. A1.1, orbit 29014). Eastward  
1025 currents at such low latitudes are missing during the other orbits of this storm period. The variations of the **ASYM/H AsyH** index reflect quite clearly the variations of the Hall current **density intensity**: it attenuates from the orbits 29012 to 29013, and increases during orbit 29014, while it decreases again during orbit 29015.

A westward current on the daytime occurs at MLat 72°–80°, beginning with orbit 29015 and con-  
1030 tinuing until orbit 29020, i.e., throughout the recovery phase and in the absence of intense substorms. The currents achieve a maximum **density strength** of  $I=1.53$  A/m during orbit 29018 at MLat 76.3°. This current is controlled by IMF By>0 and changes its direction with the IMF By orientation. It is therefore definitively a PE.

The currents in the midnight sector (Fig. A1.2, right column) are generally westward directed with

1035 weak **density intensity**. The only exception occurs during orbit 29014, where the current **density intensity** achieves  $I \sim 1.2$  A/m. This orbit coincides with the development of a very intense substorm, where the Hall current distribution is very broad with two maxima of the current **density intensity** at MLat  $61.2^\circ$  and  $73.0^\circ$ . Such a broad latitudinal distribution of the auroral luminescence, with various maxima at different latitudes, is characteristic for the recovery phase of an auroral substorm  
 1040 (Elphinstone et al., 1996). But for the present storm of 24 August 2005, the broad splitting up in latitude appeared in the Hall currents during the main phase of the storm.

Summarizing the results of Hall current observations by the CHAMP satellite during the magnetic disturbance period of 24 August 2005 in the daytime and nighttime sectors (11–13 MLT and 23–24 MLT, respectively) we conclude:

1045 For the midday sector:

- An EE with a current **density strength** of 1.37 A/m exist during the **ereation growth** phase at MLat  $\sim 73.0^\circ$  for substorms in the auroral zone with intensities of  $AL \sim -1000$  nT.
- The EE is observed at MLat  $< 60^\circ$  during the main storm phase for intense substorms with intensities of  $AL \sim -3000$  nT.
- 1050 – The variations of the EE intensities during the **ereation growth** and main phases of the storm occur synchronous with the **ASYM/H AsyH** index. Comparable variations with the **SYM/H SymH** index are not observed.
- Westward or eastward directed currents are observed during the recovery phase at  $72^\circ < MLAT < 80^\circ$  with a maximum **density intensity** of  $\sim 0.9$  A/m. Their direction is controlled by the IMF By  
 1055 component, i.e., they are in accordance with the PE.

For the midnight sector:

- As a rule, the Hall currents are westward directed during nighttime. In the concrete observations, the WE can be splitted into several parts with several maxima versus latitude.

A2 The magnetic storm of 18 June 2003

1060 Fig. A2.1 shows the variations of the **SYM/H SymH** and **ASYM/H AsyH** indices for the magnetic storm of June 18th, 2003. The storm phases are represented by the orbit numbers 16532 and 16533 for the **ereation growth** phase, 16534–16536 for the main phase, and 16537–16541 for the recovery phase. Extreme values of **SYM/H SymH** and **ASYM/H AsyH** are observed during the main phase with  $-163$  nT and  $91$  nT, respectively, while the substorm index AL achieves  $-1298$  nT. The  
 1065 CHAMP trajectories are situated during this storm period along the meridional plane of 13–14 MLT (afternoon) and 00–02 MLT (near midnight). In the daytime sector, a EE exist during the **ereation growth** phase at MLat  $\sim 67^\circ$  with  $I \sim 0.43$  A/m, and a WE at MLat  $\sim 72^\circ$  with  $I \sim 0.42$  A/m. Both electrojets are retained during the main storm phase with an EE of  $I \sim 0.8$  A/m at MLat  $\sim 62^\circ$  and a

WE of  $I \sim 0.5$  A/m at MLat  $\sim 67^\circ$ . The WE only persists during the recovery phase with  $I \sim 0.3$  A/m at MLat  $\sim 78^\circ$  (orbits 16537 and 16538). This high-latitude westward current near MLat  $\sim 77^\circ$  with  $I \sim 0.4$  A/m does not vanish till the end of the recovery phase. Such a high-latitude position of a westward current near noontime MLT gives reason to suggest that this is a polar electrojet (PE). This assumption would apply, if the IMF  $B_y$  component is negative. Indeed, the  $B_y$  component appeared to be at a steady neagative value during the orbits 16537–16541.

As a rule, the ionospheric currents in the nighttime sector are westward directed in the MLat range of  $57.8^\circ$ – $63.0^\circ$  with  $I \sim 0.5$  A/m. Only during two orbits in the ~~creation~~ growth and main phases, the current ~~density strength~~ achieved  $I \sim (1.1$ – $1.4)$  A/m.

It should be noted that this storm had relatively intense ~~SYM/H~~ SymH values, while the ~~ASYM/H~~ AsyH values remained however at a relatively low level. The EE and WE intensities were small as well.

Summarizing the results of Hall current observations by the CHAMP satellite during the magnetic disturbance period of 18 June 2003 in the daytime and nighttime sectors (13–14 MLT and 00–02 MLT, respectively) we conclude:

- The quite strong geomagnetic storm (according to the ~~SYM/H~~ SymH  $< -150$  nT index value during the main phase) is accompanied by substorms with AL up to  $-1500$  nT and with the ~~lower~~ uppermost index value for the asymmetry of the field ~~ASYM/H~~ AsyH  $< -100$  nT. The peculiarities of this storm period caused obviously the appearance of an EE in the daytime sector and a WE in the nighttime sector at MLat  $< 60^\circ$ .
- A stable PE with a current ~~density intensity~~ up to  $0.4$  A/m in westward direction persists during the recovery phase with an IMF  $B_y < 0$  nT component.

### A3 The magnetic storm of 30 May 2005

Fig. A3.1 shows the variations of the ~~SYM/H~~ SymH, ~~ASYM/H~~ AsyH, AU, and AL indices for the magnetic storm of May 30, 2005, between 02 UT and 20 UT. The vertical dotted lines indicate the time intervals of the satellite crossings over high latitudes of the Northern Hemisphere (MLat  $> 60^\circ$ ), and the numbers denote the satellite's orbit counter. Prior to the storm onset (orbits 27659 and 27660), the geomagnetic field is according to all indices, including the AL index, relatively quiet. It is recovered from  $-28.6$  nT to  $-17.3$  nT in terms of ~~SYM/H~~ SymH, from  ~~$-38$  nT to  $-18$  nT~~  $37.8$  nT to  $17.8$  nT for ~~ASYM/H~~ AsyH, and from  $-40$  nT to  $0$  nT with respect to the AL index. These changes correspond to a recovery process toward a quiet time level after the previous disturbance.

The main phase of the magnetic storm starts with a steady increase of ~~SYM/H~~ SymH from  $-29$   $-28.6$  nT during orbit 27661, a jump-like increase from  $44.5$  nT to  $104.2$  nT in ~~ASYM/H~~ AsyH during the same overflight and continues with an ~~in~~ decrease of ~~SYM/H~~ SymH to  $-118.4$  nT during orbit 27665. The peak values of ~~ASYM/H~~ AsyH and AL during the main storm phase are  $162.1$  nT



and  $-1200\text{ nT}$ , respectively. The recovery phase takes place during the orbits 27666 and 27667, after  
1105 which during the orbit 27668 the appearance of a new disturbance is recorded (according to the AL  
and **SYM/H SymH** indices). The ascending CHAMP trajectory during the storm goes along the 19–  
21 MLT meridian (evening), while the descending orbit section is along the 06–09 MLT meridian in  
the morning sector. Fig. A3.2 shows the direction and the **density strength** of the Hall currents for  
the evening (left side) and morning (right side) sectors.

1110 During the orbits prior to the beginning of the main phase, the Hall current is either missing in the  
evening sector or exists only in terms of a distributed eastward current with maximum densities of  
 $J \sim 0.3\text{ A/m}$  at  $\text{MLat} \sim 66^\circ$ . In the morning sector, a WE is recorded with  $J \sim 0.9\text{ A/m}$  at  $\text{MLat} \sim 80^\circ$  and  
MLT  $\sim 09$  hours. The existence of such intense currents during daytime hours at such high latitudes  
during relatively quiet geomagnetic conditions is unusual. A reasonable explanation might be the  
1115 assumption that this current concerns the PE. In this case, the orbits investigated should occur during  
conditions of  $\text{IMF } B_y < 0\text{ nT}$ . Indeed, according to Fig. A3.1 a quite stable negative  $\text{IMF } B_y \sim -$   
 $18\text{ nT}$  is observed prior to the main storm phase. The beginning of the main phase (orbit 27661)  
is characterized by the appearance of two currents in the evening sector: the EE with  $J \sim 0.6\text{ A/m}$  at  
 $\text{MLat} \sim 63^\circ$  and the WE with  $J \sim 0.3\text{ A/m}$  at  $\text{MLat} \sim 68^\circ$ . In the course of the storm, the EE attains  
1120 a **density strength** of  $J \sim 0.7\text{ A/m}$ , shifting equatorward until  $\text{MLat} \sim 80^\circ$ . The displacement in  $\text{MLat}$   
toward the equator reflects the more general tendency, according to which the electrojets move  
more equatorward with increasing current  $J$ . The current **density intensity** in the WE retains at  
 $J \sim 0.4\text{ A/m}$ . In the morning sector, the current stays at  $\text{MLat} \sim 70^\circ$ , and its current **density strength**  
during orbit 27661 is kept at  $J \sim 0.4\text{ A/m}$ . This is obviously the first appearance of an auroral WE in  
1125 the morning sector. The WE at auroral latitudes increases during the subsequent orbits and attains  
 $1.5\text{ A/m}$  during orbit 27665 at  $\text{MLat} \sim 64^\circ$ . The recovery phase during orbit 27667 is characterized  
by a westward current with  $J \sim 1.0\text{ A/m}$  in the morning sector at  $\text{MLat} \sim 68^\circ$  and a weaker current  
with  $J \sim 0.3\text{ A/m}$  at  $\text{MLat} \sim 63^\circ$ . In the course of the storm, the current **density intensity**  $J$  in the  
morning sector exceeds significantly the Hall current **density intensity** values of the same orbit in the  
1130 evening sector.

Summarizing the results of Hall current observations by the CHAMP satellite during the magnetic  
disturbance period of 30 May 2005 in the dusk and dawn sectors (19–21 MLT and 06–09 MLT,  
respectively) we conclude:

- 1135 – Two auroral Hall currents (EE and WE) exist in the evening, and one current only (WE) in the  
morning sector;
- The currents are positioned, as a rule, at latitudes  $\text{MLat}$  of the auroral zone ( $63^\circ$ – $68^\circ$ ). During  
the main phase, the current can be shifted to  $\text{MLat} \sim 58.5^\circ$ ;
- In the evening sector, the position of the EE is more equatorward than the WE;
- During early evening hours, the Hall current **density strength** of the EE exceeds the WE current

1140 **density intensity**, and in the morning hours the WE current **density intensity** is larger than during the evening;

- The recovery process toward the quiet-time level can be accompanied at by late evening or polar electrojet (PE) at MLat $\sim$ 80° in the late morning hours of the PE with J $\sim$ 0.8 A/m.

#### A4 The magnetic storm of 15 May 2005

1145 Fig. A4.1 shows the variations of the **SYM/H SymH**, **ASYM/H AsyH**, and IndN indices, as well as the IMF By and Bz components and the solar wind velocity in the interval 00–23 UT for the magnetic storm of May 15, 2005. The main phase of the magnetic storm takes place during the orbits 27426 and 27427 with a **SYM/H SymH** index value of  $\sim$ 274–274.5 nT, an **ASYM/H AsyH** of  $\sim$ 186.1 nT, and AL *sim*-1700 nT. The orbits 27423 and 27424 prior to the main phase occur during weakly  
1150 disturbed magnetic field conditions with **SYM/H SymH**  $\sim$ 50 nT and **ASYM/H AsyH**  $\sim$ 75–16 nT. During orbit 27425 with **SYM/H SymH**  $\sim$ 48.8 nT, the **ASYM/H AsyH** index increases strongly to  $\sim$ 121.3 nT, which appears to be the onset of an intense magnetic storm. The recovery phase takes place during the orbits 27428 and 27432, during which occurs a steady decrease of the **SYM/H SymH** index to  $\sim$ 125.2 nT and of the **ASYM/H AsyH** index value to  $\sim$ 70.1 nT. The ascending  
1155 CHAMP trajectory during the storm spread along the 20–22 MLT meridian, and the descending trajectory is along the 08–10 MLT meridian in the morning sector. Fig. A4.2 shows the direction and the **density strength** of the Hall currents for the evening (left side) and morning (right side) sectors.

The current **density strength** for the EE during orbit 27425 is with  $\sim$ 0.4 A/m quite small in the  
1160 evening sector prior to the main phase. Both an EE and a WE exist during the main phase with J $\sim$ 0.6 A/m. The EE shifts on average to a MLat of  $\sim$ 52.5° with **SYM/H SymH**  $\sim$ 250 nT. The Hall currents are practically absent during the recovery phase.

In the evening sector, the currents turn out to have difficult characteristics, changing with the storm phases. A WE at MLat $\sim$ 72° with J $\sim$ 1.0 A/m is recorded during the magnetically quiet period prior  
1165 to the main phase. With the development of the main phase, the WE shifts to MLat $\sim$ 61°. During the recovery phase, the WE decays at auroral latitudes, but in the latitudinal range 77°<MLat<80° an EE appears with J $\sim$ 1.0 A/m (orbits 27428–27431). The orbits with an EE coincide temporally with an interval of IMF By>0 nT in the solar wind (Fig. A4.1). All characteristic features of the PE are therefore present here. During orbit 27433, the direction of the current changes to WE. This is  
1170 accompanied by a corresponding change of the IMF By orientation as can be seen in Fig. A4.1.

The characteristic features of this storm are the following:

- The quiet-time level of the magnetic field variations prior to the storm main phase can be describes as missing or unimportant intensities of the EE and WE Hall currents in the evening sector, while in the morning sector exists only the WE at auroral latitudes.

- 1175      – During the main phase of this intense storm with a **SYM/H SymH** index of  $\sim -250$  nT in the evening sector, the WE shifts to MLat $\sim 52.5^\circ$ , and the WE to MLat $\sim 54.0^\circ$ .
- A PE appears during the recovery phase in the late morning hours at  $77^\circ < \text{MLat} < 80^\circ$ , where the Hall currents are controlled by the direction of the IMF By component.

#### A5 The magnetic storm of 18 August 2003

- 1180 Fig. A5.1 shows the variations of the **SYM/H SymH**, **ASYM/H AsyH**, **AU**, and **AL** indices, as well as the IMF By and Bz components in the interval 00–23 UT for the magnetic storm of August 18, 2003. The main phase of the magnetic storm takes place during the orbits 17482–17489 with peak values of **SYM/H SymH** and **ASYM/H AsyH** of  $\sim -1353.8$  nT and  $\sim -101.4$  nT, respectively, and an **AL** value of  $\sim -1400$  nT. During the orbits 17480 and 17481 prior to the main phase the
- 1185 values of **SYM/H SymH** and **ASYM/H AsyH** are  $\sim -18.4$  nT to  $-43.3$  nT and  $\sim -72.0$ – $-498.8$  nT, and during the recovery phase in the course of orbits 17490–17493 they amount to  $\sim -115.4$  nT and  $\sim -56.7$  nT, respectively. The CHAMP trajectories during the storm spread along the 07–09 MLT meridian (morning) and along the 19–21 MLT meridian (evening). Fig. A5.2 shows the direction and the **density strength** of the Hall currents for the morning (left side) and evening (right side) sectors.
- 1190 The characteristic peculiarities of the spatial-temporal distribution of the FACs during this storm concur with those described for the other storms. During the main phase in the evening sector, there exists, as a rule, an EE. The EE appears at MLat $\sim 66.5^\circ$  with  $J \sim 0.6$  A/m, and shifts then equatorward to MLat $\sim 58.8^\circ$  with  $J \sim 1.0$  A/m during orbit 17486. A WE exists in the morning sector at auroral latitudes of  $61^\circ < \text{MLat} < 65^\circ$  with  $J \sim 1.2$  A/m. A weak distributed eastward current in the polar cap
- 1195 persists due to the closure of parts of the electrojets across the near-polar region.

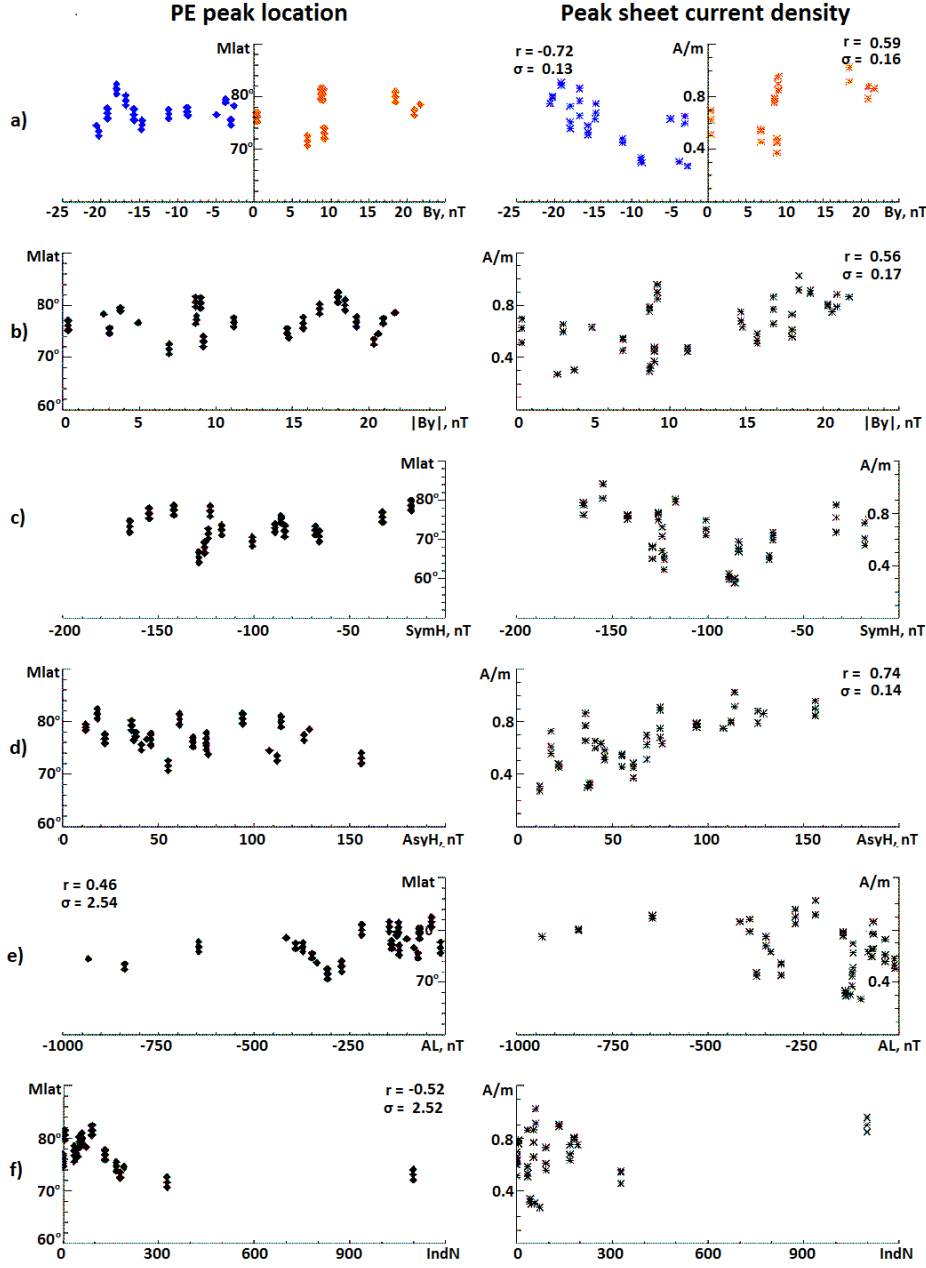


**Fig. 3.** Dependence of the magnetic latitude MLat (degrees) position of the peak (left column) and its **density intensity** ( $I$  in A/m, right column) of the Hall current in the polar electrojet (PE) on the IMF  $B_y$  component (a) and its magnitude (b), on the geomagnetic activity indices **SYM/H** SymH (c), **ASYM/H** AsyH (d), AL (e), and the solar wind coupling function IndN (f). **The blue and red data points indicate westward and eastward currents, respectively.** For the cases of correlations with  $r > 0.46$ , the correlation coefficients ( $r$ ) and the dispersion ( $\sigma$ ) according to a linear regression are shown as labels.

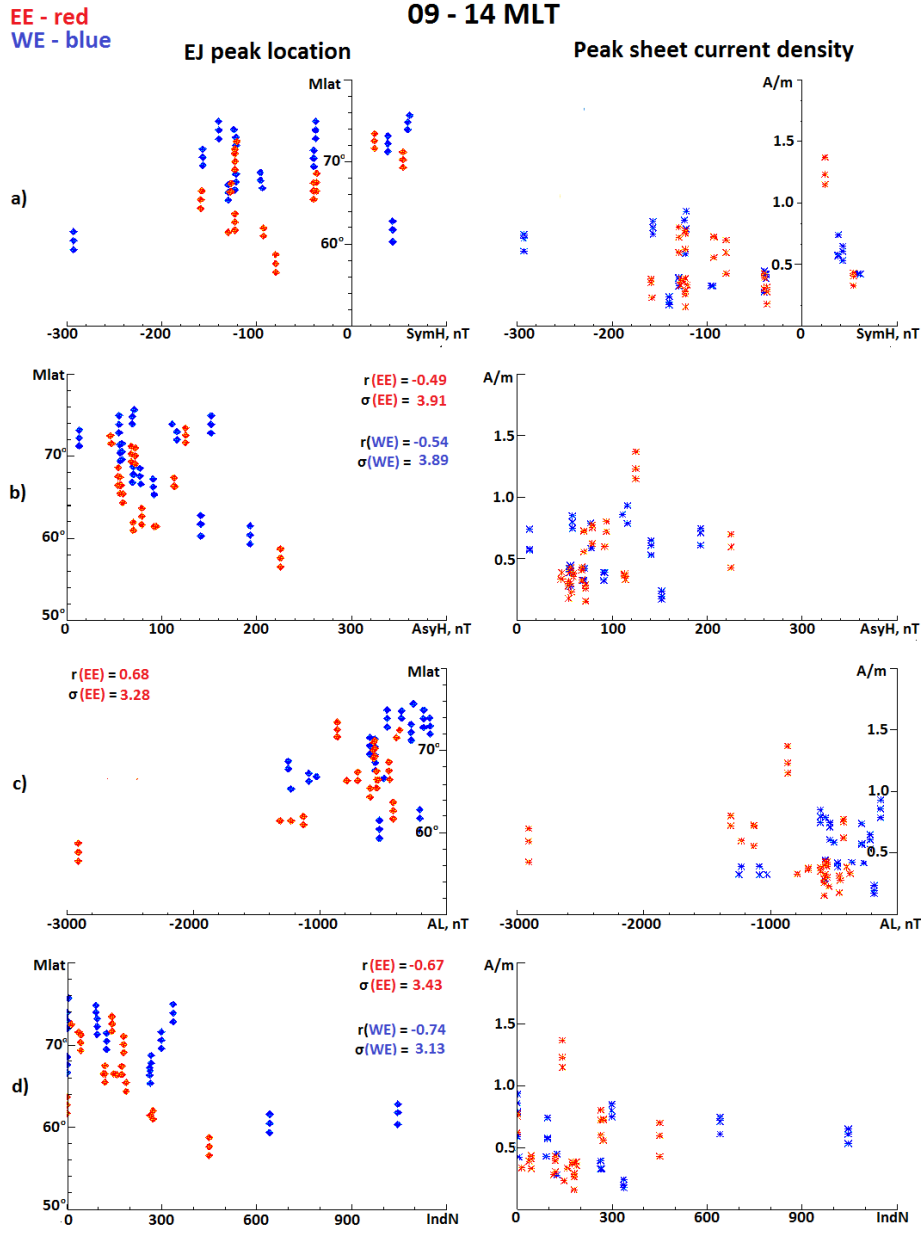


**Fig. 4.** Daytime sector (09–14 MLT): Dependence of the magnetic latitude MLat (degrees) position of the peak (left column) and of the **density intensity** ( $I$  in A/m, right column) of Hall current in the WE (blue) and EE (red) on the geomagnetic activity indices **SYM/H** SymH (a), **ASYM/H** AsyH (b), AL (c), and the solar wind coupling function IndN (d). For the cases of correlations with  $r > 0.46$ , the correlation coefficients ( $r$ ) and the dispersion ( $\sigma$ ) according to a linear regression are shown as labels.

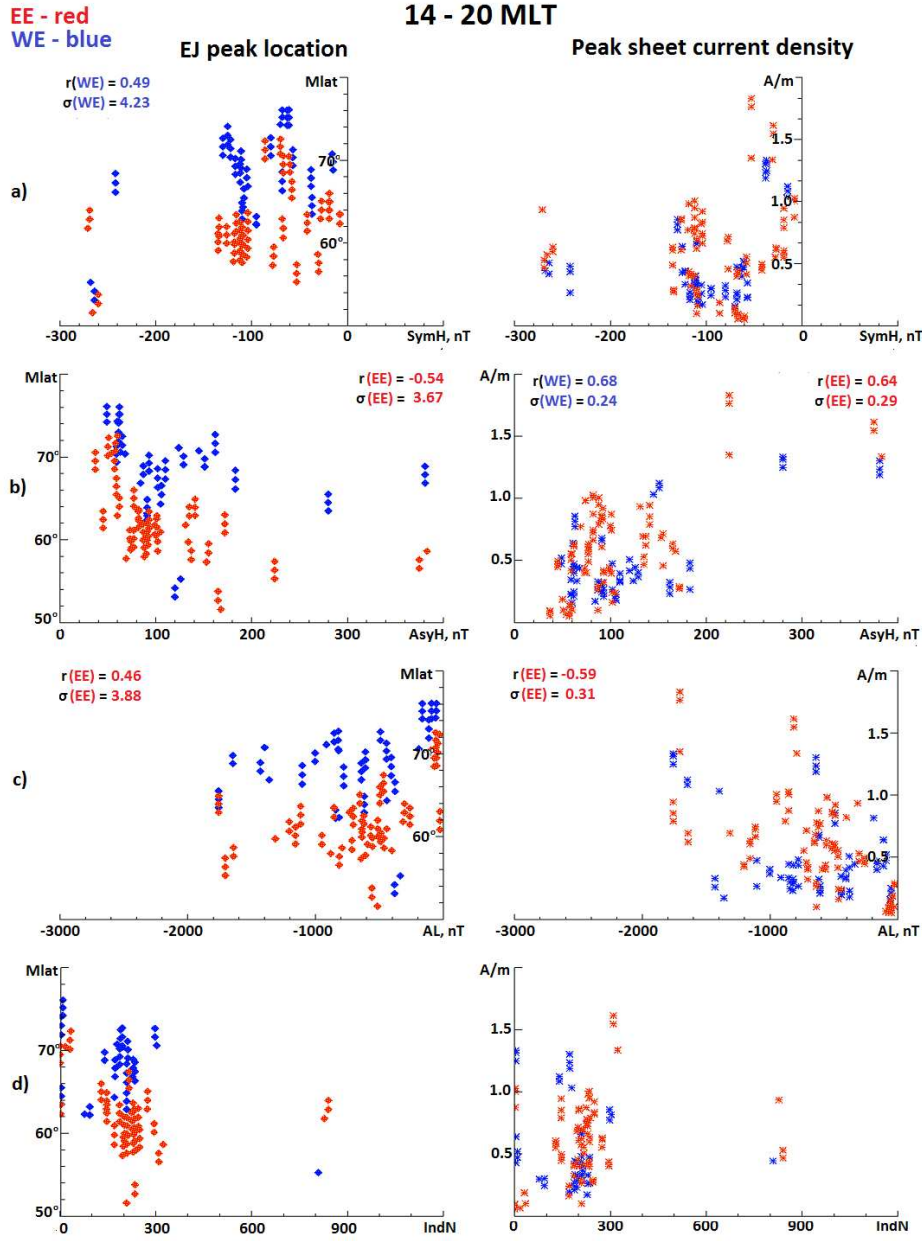


**Fig. 5.** The same as in Fig. 4, but for the evening sector (14–21 MLT).

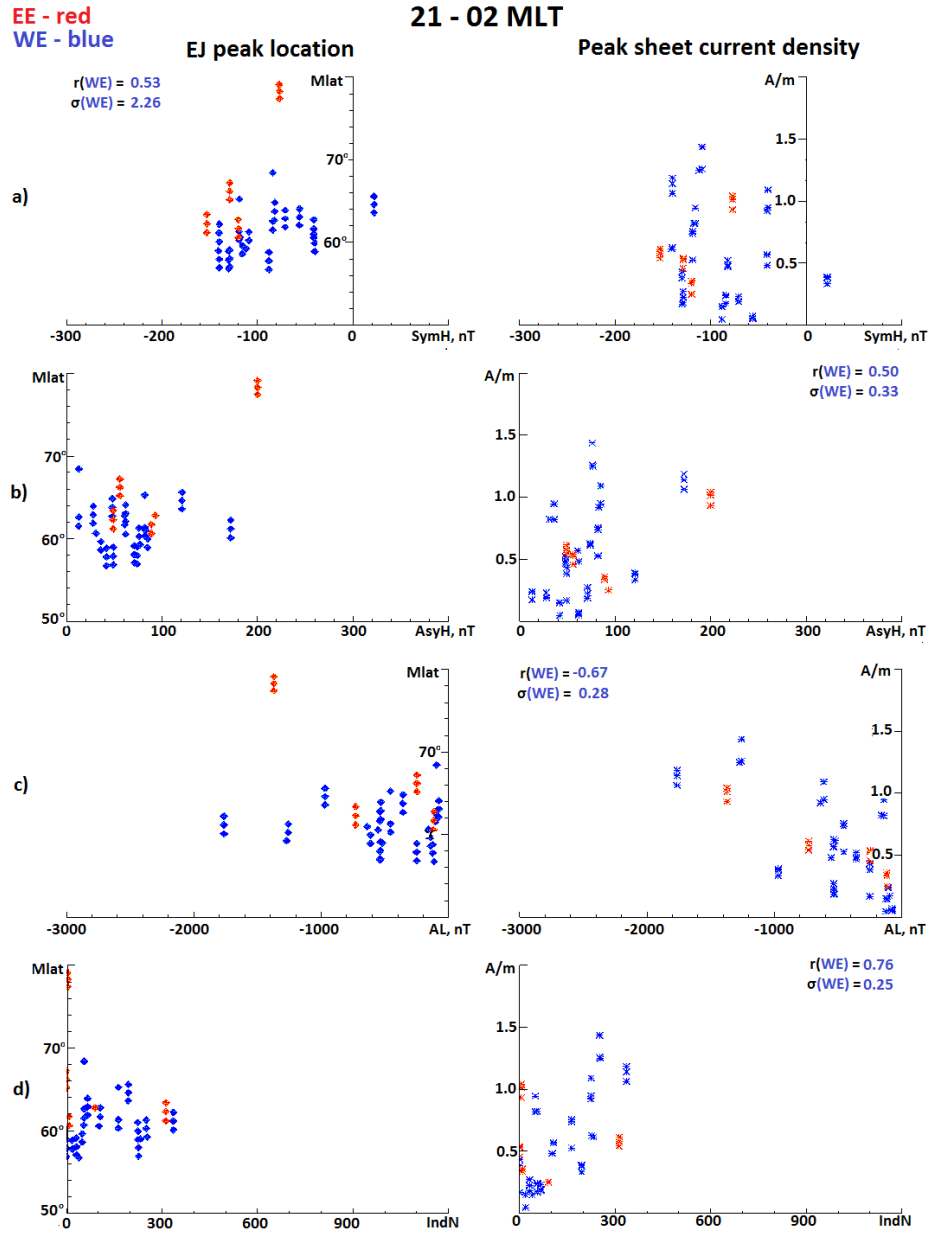


**Fig. 6.** The same as in Fig. 4, but for the midnight sector (21–02 MLT).



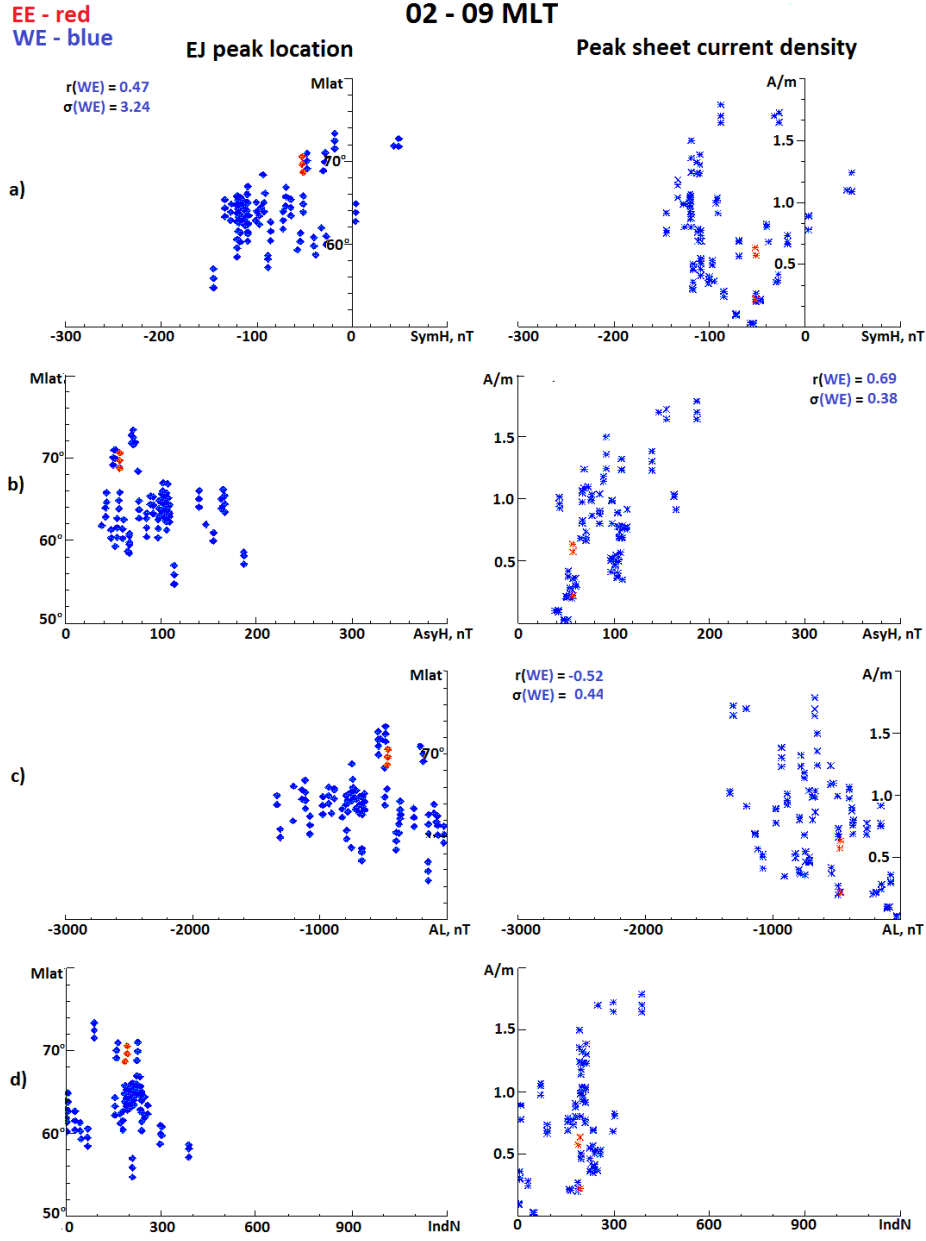


**Fig. 7.** The same as in Fig. 4, but for the morning sector (02–09 MLT).

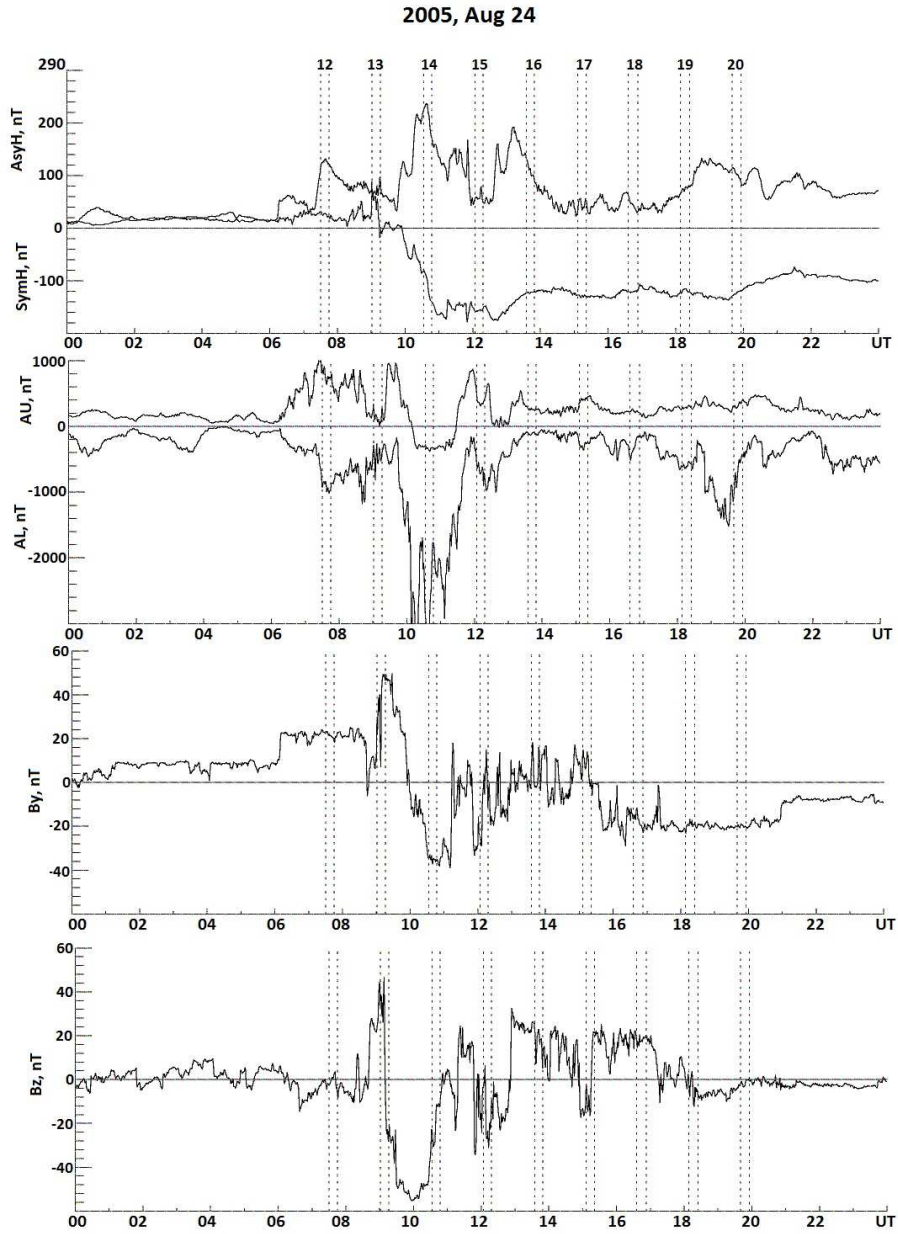


**Fig. A1.1.** One-minute values of the **ASYM/H** AsyH, **SYM/H** SymH, **AU**, and **AL** indices and of the **By** and **Bz** components of the IMF for the storm of 24 Aug 2005 (analysis interval from 07:00–20:00 UT, orbits 29012–29020). The time of each orbit and its orbit number are indicated as in Fig. 1 of the paper.

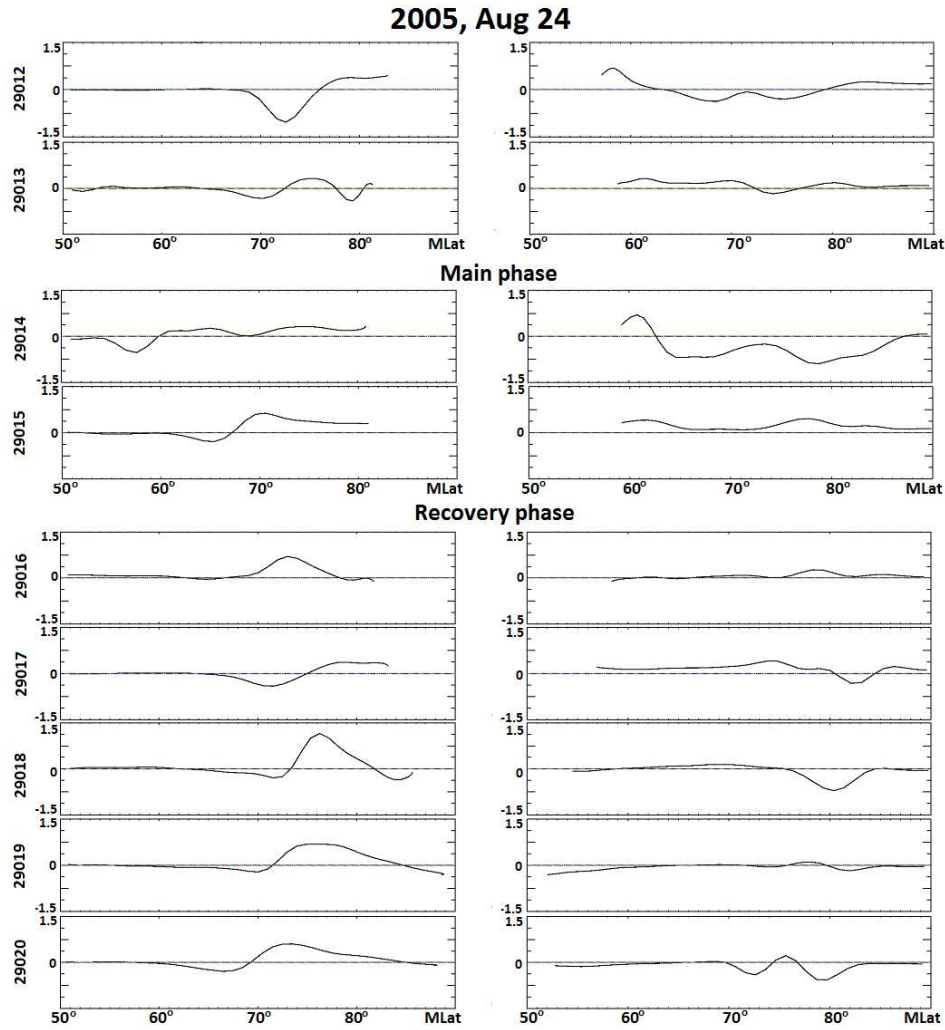


**Fig. A1.2.** Direction and **density intensity** values of the Hall current along the satellite orbit at the dayside (left column, 11–13 MLT, corresponding to the ascending section of the orbit) and nightside sectors (right column, 23–24 MLT, descending orbit section). Positive currents denotes eastward current for the descending orbit section, and, **accordingly**, westward current for the ascending section, **respectively**.

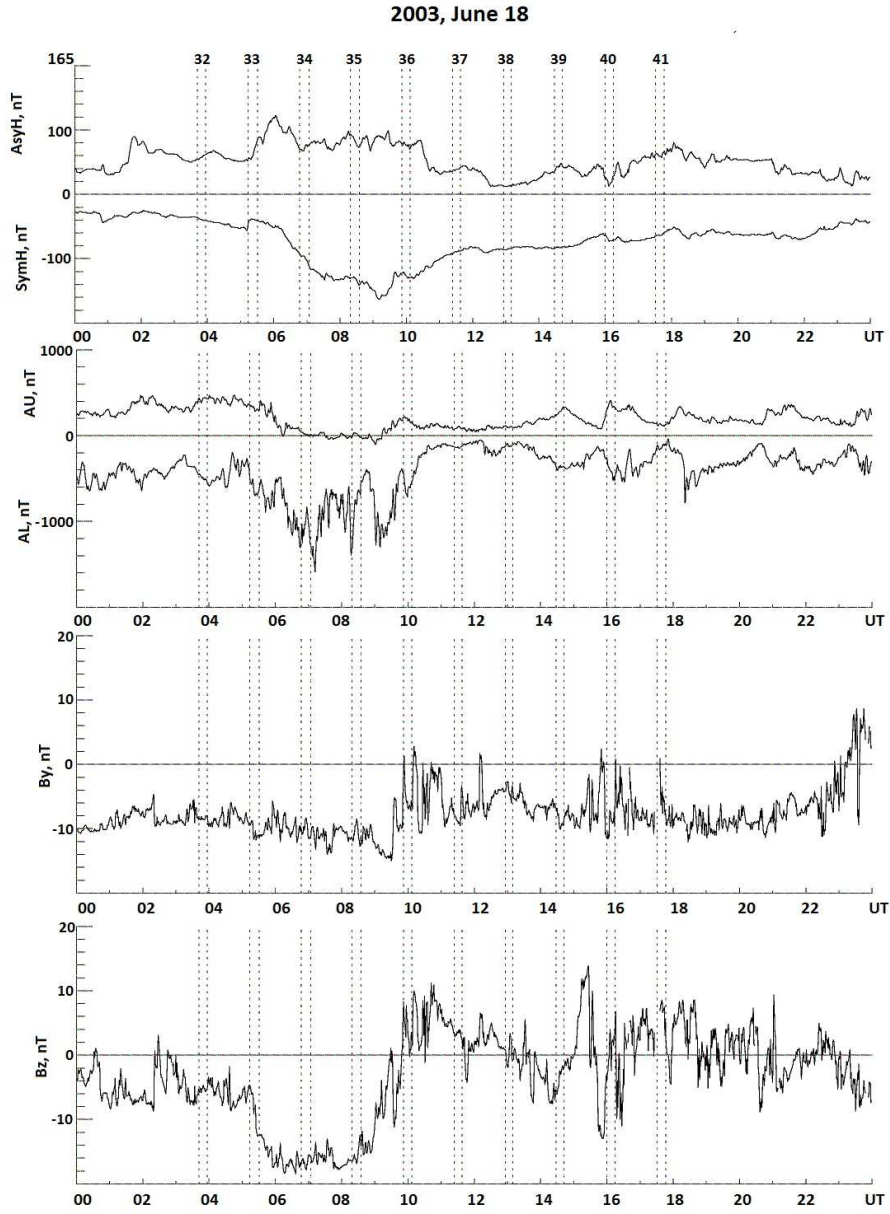


**Fig. A2.1.** One-minute values of the **ASYM/H** AsyH, **SYM/H** SymH, **AU**, and **AL** indices and of the By and Bz components of the IMF for the storm of 18 June 2003 (analysed interval from 03:00–18:00 UT, orbits 16532–16541). The time of each orbit and its orbit number are indicated as in Fig. 1 of the paper.

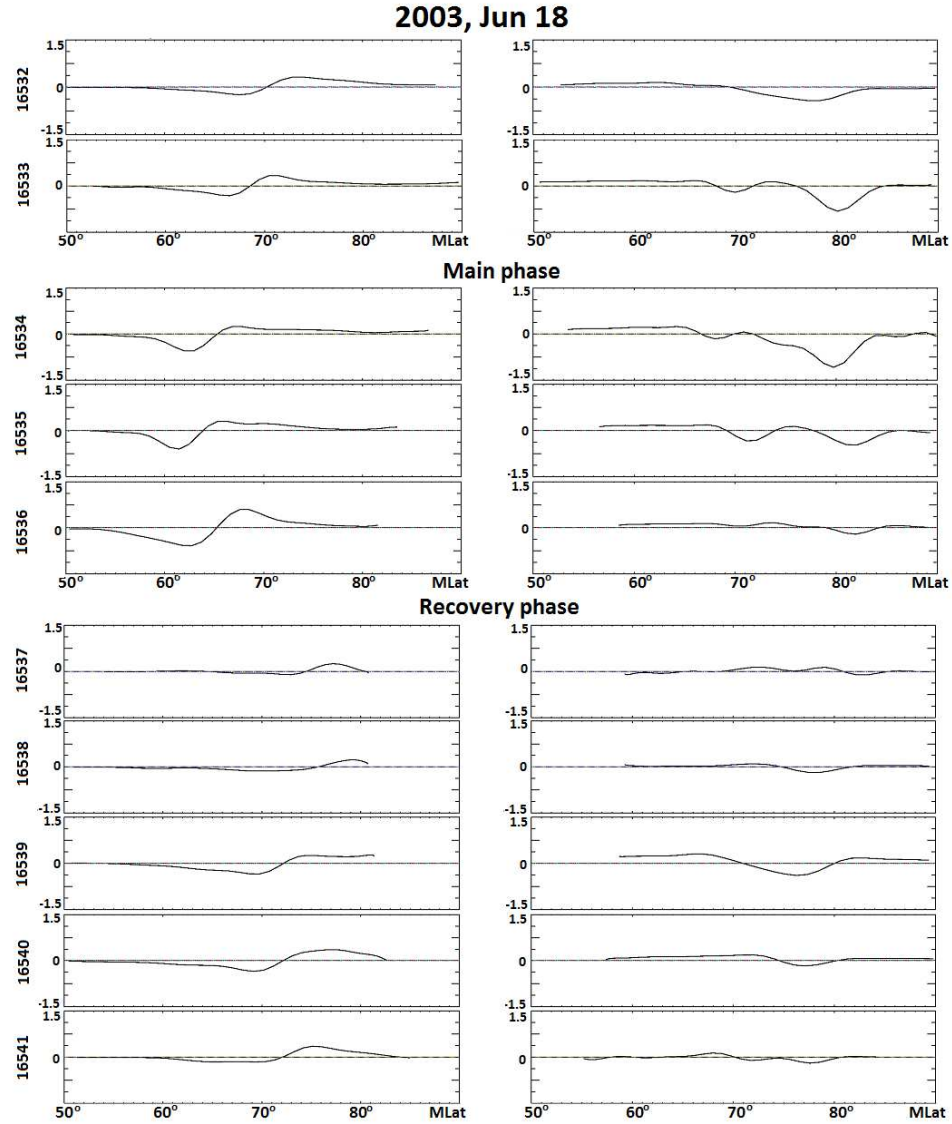


**Fig. A2.2.** Direction and **density intensity** values of the Hall current along the satellite orbit at the dayside (left column, 12–16 MLT, corresponding to the ascending section of the orbit) and nightside sectors (right column, 00–04 MLT, descending orbit section). Positive currents denotes eastward current for the descending orbit section, and, **accordingly**, westward current for the ascending section, **respectively**.

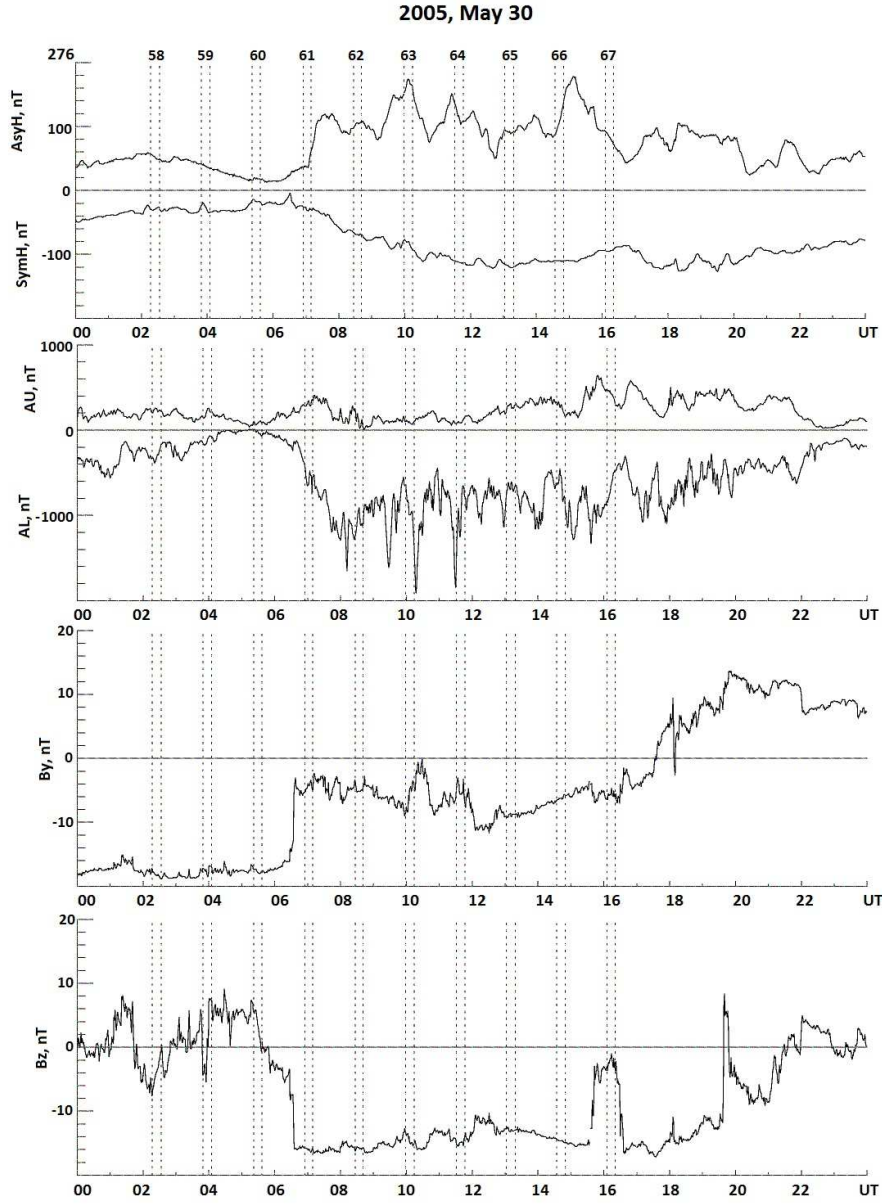


**Fig. A3.1.** One-minute values of the **ASYM/H** AsyH, **SYM/H** SymH, **AU**, and **AL** indices and of the **By** and **Bz** components of the IMF for the storm of 30 May 2005 (analysis interval 02:00–17:00 UT, orbits 27658–27667). The time of each orbit and its orbit number are indicated as in Fig. 1 of the paper.



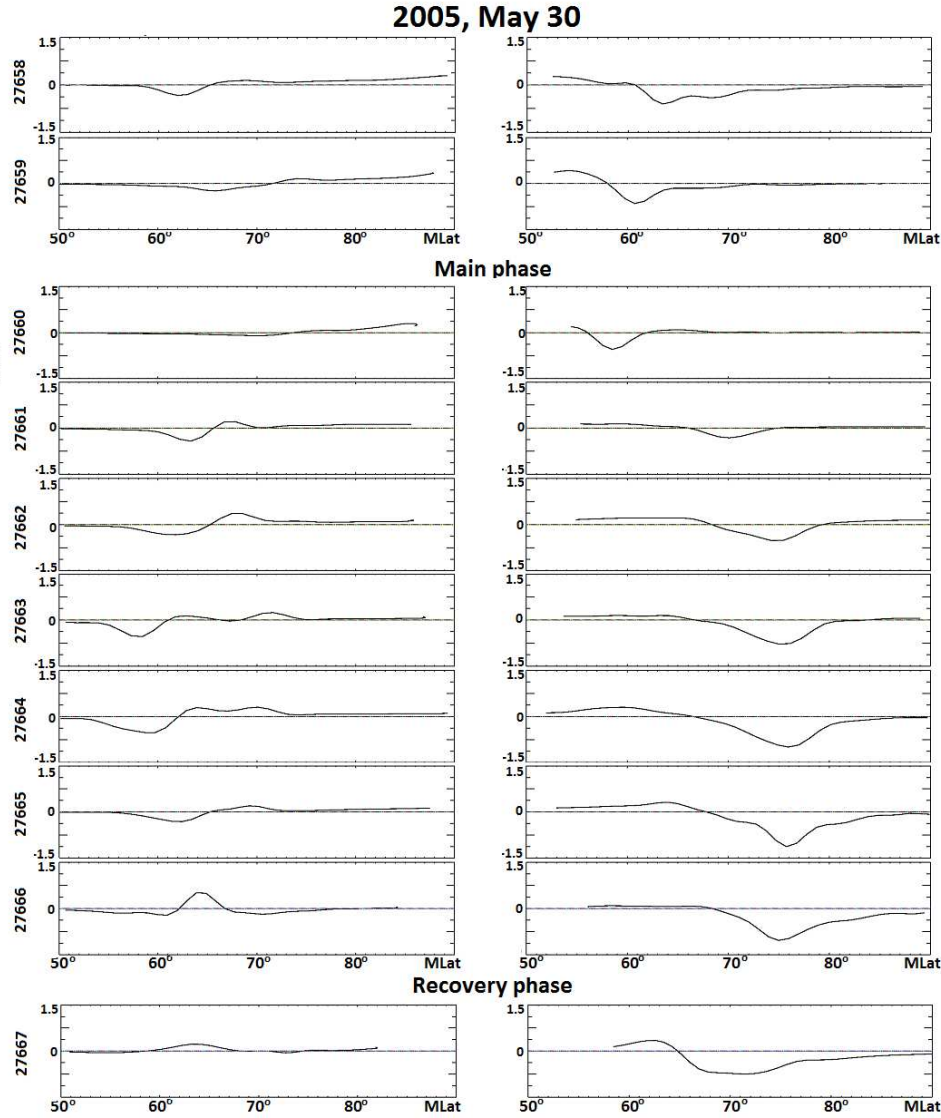


**Fig. A3.2.** Direction and **density intensity** values of the Hall current along the satellite orbit at the duskside (left column, 19–21 MLT, corresponding to the ascending section of the orbit) and dawnside sectors (right column, 06–09 MLT, descending orbit section). Positive currents denote an eastward current flow for the descending orbit section, and, **accordingly**, westward current for the ascending section, **respectively**.



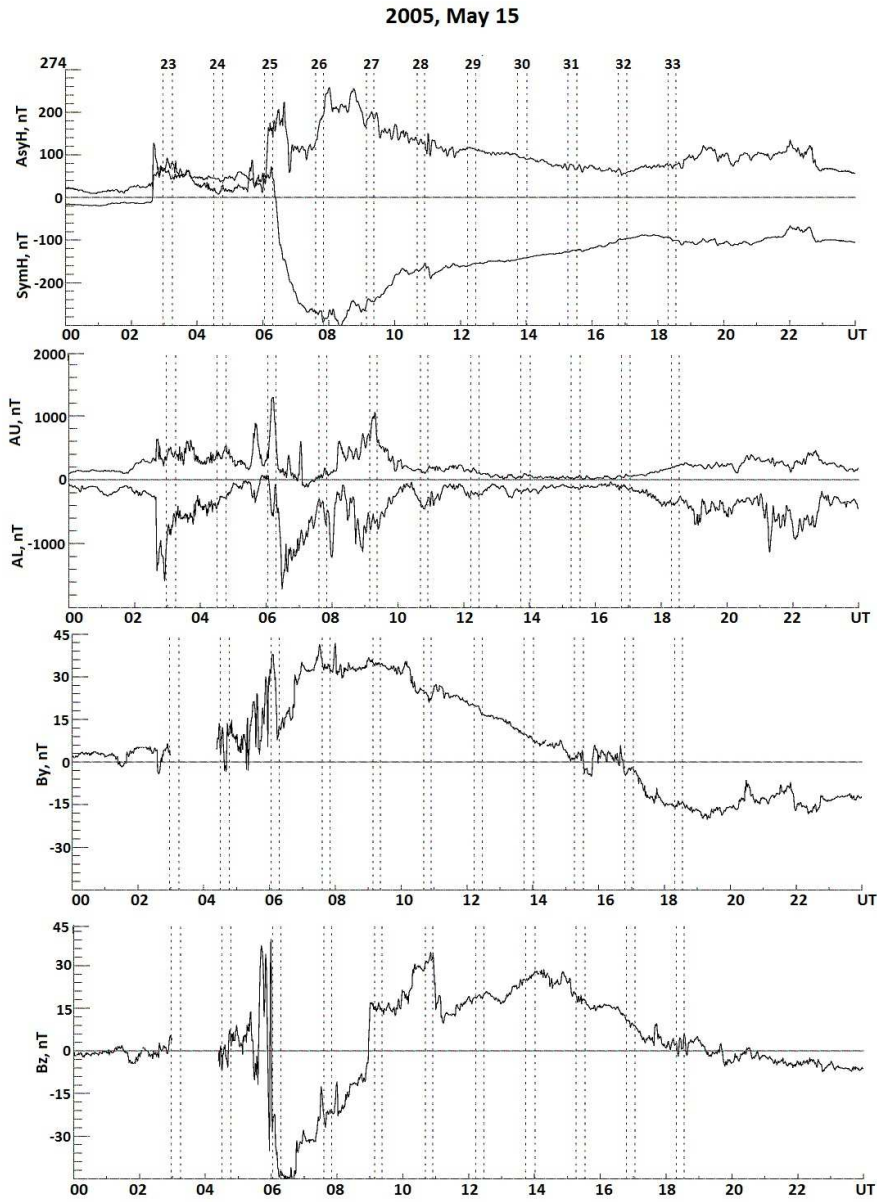


**Fig. A4.1.** One-minute values of the **ASYM/H** AsyH, **SYM/H** SymH, **AU**, and **AL** indices and of the By and Bz components of the IMF for the storm of 15 May 2005 (analysis interval 002:00–19:00 UT, orbits 27423–274323). The time of each orbit and its orbit number are indicated as in Fig. 1 of the paper.

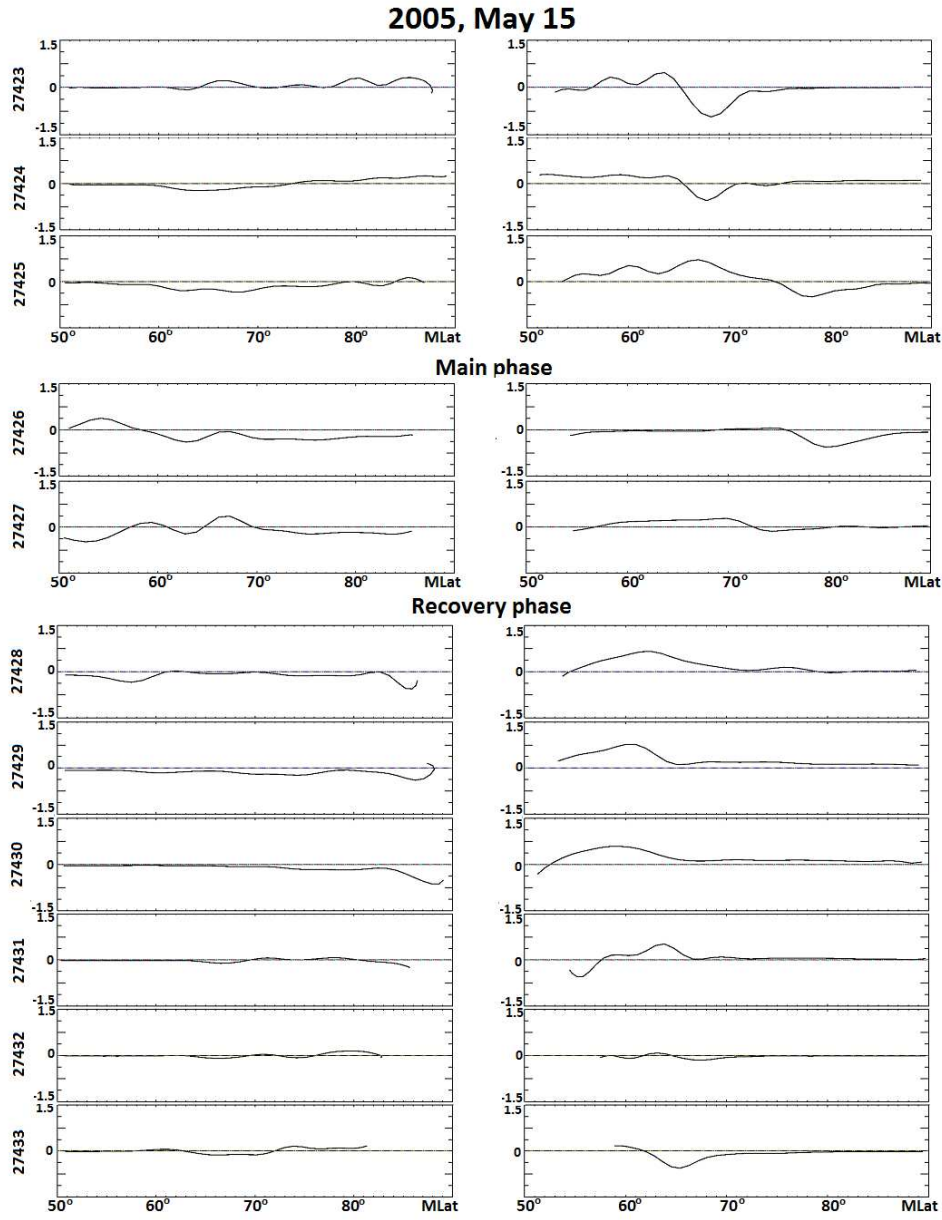


**Fig. A4.2.** Direction and **density intensity** values of the Hall current along the satellite orbit at the duskside (left column, 20–22 MLT, corresponding to the ascending section of the orbit) and dawnside sectors (right column, 08–10 MLT, descending orbit section). Positive currents denote an eastward current flow for the descending orbit section, and, **accordingly**, westward current for the ascending section, **respectively**.

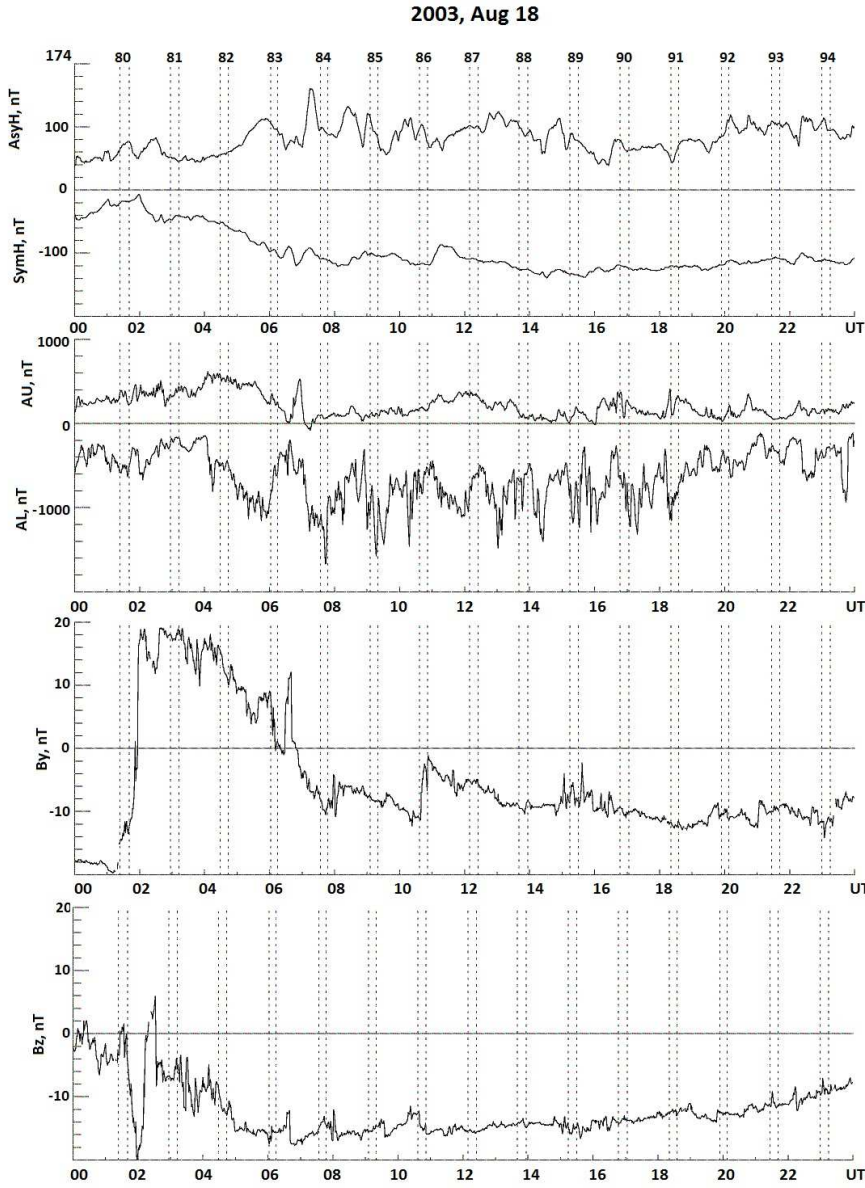


**Fig. A5.1.** One-minute values of the **ASYM/H** AsyH, **SYM/H** SymH, **AU**, and **AL** indices and of the **By** and **Bz** components of the IMF for the storm of 18 Aug 2003 (analysis interval 00:00–23:00 UT, orbits 17480–17494). The time of each orbit and its orbit number are indicated as in Fig. 1 of the paper.

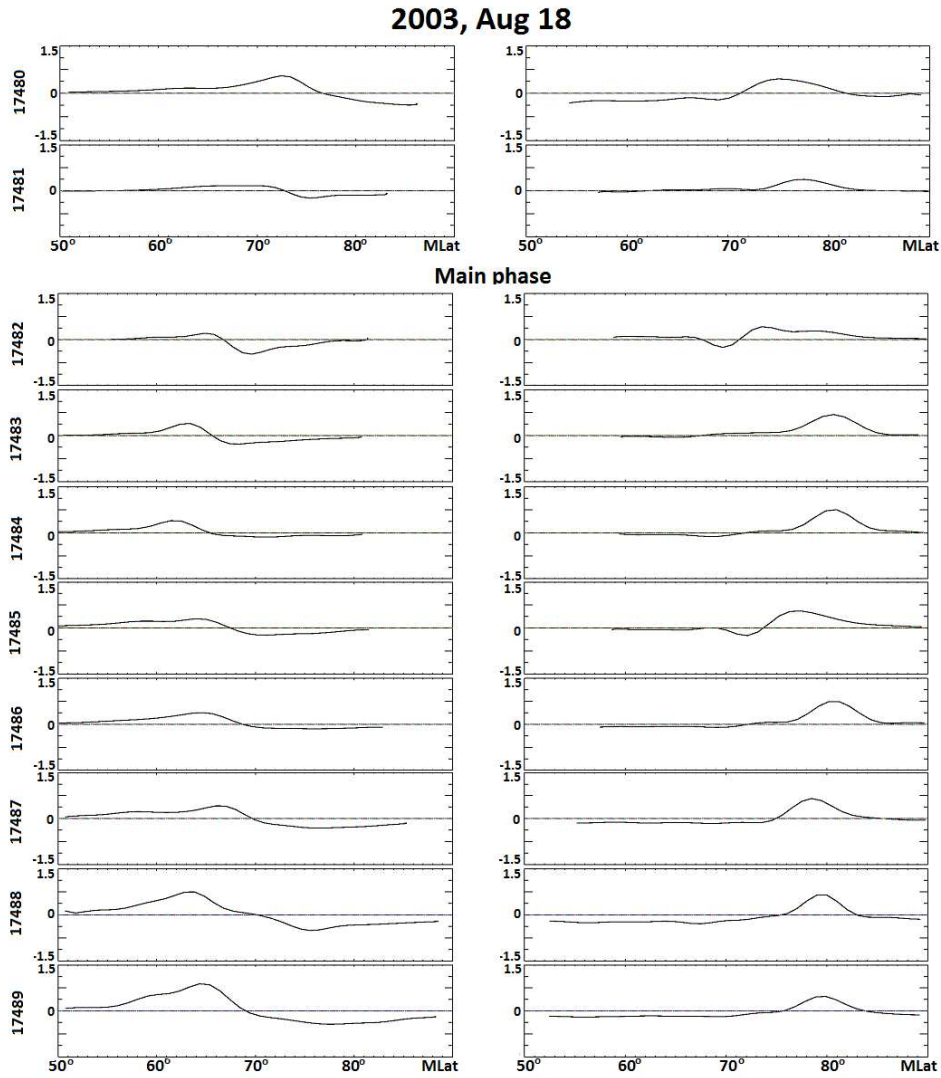


**Fig. A5.2.** Direction and ~~density~~ intensity values of the Hall current along the satellite orbit at the dawnside (left column, 07–09 MLT, corresponding to the ascending section of the orbit) and duskside sectors (right column, 19–21 MLT, descending orbit section). Positive currents denote an eastward current flow for the descending orbit section, and, ~~accordingly,~~ westward current for the ascending section, ~~respectively.~~